DOT/FAA/TC-20/32

Federal Aviation Administration
William J. Hughes Technical Center
Aviation Research Division
Atlantic City International Airport
New Jersey 08405

Unmanned Aircraft Systems (UAS) Lithium Batteries Cell and Electrical Energy Storage System Safety

September 2020

Final Report

U.S. Department of Transportation
Federal Aviation Administration

NOTICE

This report is available at the Federal Aviation Administration William J. Hughes Technical Center's Full-Text Technical Reports page: actlibrary.tc.faa.gov in Adobe Acrobat portable document format (PDF).

Form DOT F 1700.7 (8-72) Reproduction of completed page authorized

1. Report No.	2. Government Accession No.	3. Recipient's Catalog No.
DOT/FAA/TC-20/32		

4. Title and Subtitle	5. Report Date
FAA Aircraft Battery Safety Testing Program	September 2020
	6. Performing Organization Code

7. Author(s)	8. Performing Organization Report No.
DNV GL: Aditya Rohilla, Davion Hill, Sachi Jayasuriya, Mohammed Muthalib, Wenbo Zhang Steve Cummings (Nexceris), Timothy Riley (Pyrophobic Systems Limited), Mahesh Bailakanavar (Thornton Tomasetti)	

9. Performing Organization Name and Address	10. Work Unit No. (TRAIS)
DNV GL ENERGY INSIGHTS USA INC 1400 RAVELLO DR KATY TX 77449-5164	11. Contract or Grant No. DTFACT-16-C-00042

12. Sponsoring Agency Name and Address	13. Type of Report and Period Covered
Federal Aviation Administration William J. Hughes Technical Center Building 300, Fourth Floor Atlantic City, New Jersey 08405-0001	Final Report
	14. Sponsoring Agency Code N6942K7M

15. Supplementary Notes

The Federal Aviation Administration William J. Hughes Technical Center Aviation Research Division COR was Michael Walz

16. Abstract

The purpose of this research was to study and develop technology, and provide supporting data for industry standards to reduce the risks associated with the installation, operation, and in-service maintenance of lithium batteries. The project focused on electrical energy storage systems to be installed and used on aircrafts.

Through this work, DNV GL has tested and qualified a novel battery system that applies to commercial interests for unmanned aircraft systems with the following advancements: passive thermal containment technologies from Pyrophobic Systems, LLC, which mitigate cascading thermal runaway and contain high energy release, and off-gas sensing from Nexceris that provides early warning of a failure and battery prognostic functions.

17. Key Words	18. Distribution Statement
Lithium Batteries, Energy Storage Systems, Aircraft Battery Safety	This document is available to the U.S. public through the National Technical Information Service (NTIS), Springfield, Virginia 22161. This document is also available from the Federal Aviation Administration William J. Hughes Technical Center at actlibrary.tc.faa.gov.

19. Security Classif. (of this report)	20. Security Classif. (of this page)	21. No. of Pages	22. Price
Unclassified	Unclassified	77	

Acknowledgements

DNV GL gratefully acknowledges the financial support provided by FAA; the technical discussions and feedback from Program Manager Michael Walz; the administrative support from Contracting Officer Karen Mercer; and technical support from Nick Warner (Energy Storage Response Group), Victoria Carey (New Jersey Economic Development Authority), and contributing staff from Nexceris, Pyrophobic Systems Limited and Thornton Tomasetti.

Contents

Figures

Tables

Acronyms

Acronym	Definition
1D	One-dimensional
3D	Three-dimensional
AAM	Advanced aerial mobility
BMS	Battery Management System
C2	Command and Control
CAB	Commercial Advisory Board
CFD	Computational fluid dynamics
CFR	Code of Federal Regulations
CID	Current interrupt devices
DAA	Detect and avoid
DNV GL	DNV GL Energy Insights USA, Inc.
DOD	Depth of discharge
DOT	Department of Transportation
EAU	Estimated annual usage
EIA	Energy Information Administration
EPA	Environmental Protection Agency
eVTOL	Electric vertical take-off and landing
FAA	Federal Aviation Administration
FTIR	Fourier Transform Infrared Spectroscopy
HCl	Hydrogen Chloride
HCN	Hydrogen Cyanide
HF	Hydrogen fluoride
IEC	International Electrotechnical Commission
LBAC	Large battery abuse testing chamber
LEL	Lower explosive limit
Li-ion	Lithium Ion
$LiPF_6$	Lithium Hexafluorophosphate
NAVSEA	Naval Sea Systems Command
NFPA	National Fire Protection Agency
NiCd	Nickel cadmium
NMC	Nickel manganese cobalt

Acronym	Definition
NY-BEST	New York Battery & Energy Storage Technology
OGM	Off-gas monitor
PVC	Polyvinyl chloride
PVDF	Polyvinylidene fluoride
RTCA	Radio Technical Commission for Aeronautics
SOC	State of charge
TM	Tubular manifold
UAM	Urban air mobility
UAS	Unmanned aircraft systems
UL	Underwriters Laboratories
UN	United Nations
UTM	UAS Traffic Management
VOC	Volatile organic compound

Executive summary

The Federal Aviation Administration (FAA) retained DNV GL Energy Insights USA, Inc. (DNV GL) to research, develop, and test a prototype technology intended to reduce the hazards associated with the installation, operation, and in-service maintenance of Lithium Batteries. Through this work, DNV GL researched industry standards, assessed various subcomponents and mitigative systems, and qualified a novel battery system through intensive testing and data analysis that applies to commercial interests for unmanned aircraft systems. The prototype system included the following advancements: passive thermal containment technologies from Pyrophobic Systems, LLC, which mitigate cascading thermal runaway and contain high energy release, and off-gas detection from Nexceris that provides early warning of a failure and battery prognostic functions. The study was comprised of various tasks consisting of establishing a design philosophy for the battery module, performing basic cell block testing, using data from testing to produce models of the cell block design, testing, and validating the battery module prototype.

First, DNV GL performed a literature review to investigate general hazards that threaten all electrochemical energy storage devices, discussed the need for hazards to be appropriately managed and mitigated, and presented a review of code precedents that are relevant to battery permitting. Then, battery solution design criteria were developed to inform dimensions of the battery module, cell configuration, thermal and ventilation management, battery management system (BMS) controls for preventing electrical abuse and integration of intumescent material and off-gas monitoring technologies. An estimate of materials and costs was developed for the Commercial Advisory Board (CAB) and functional requirements for adapting an existing system to new system designs.

Second, DNV GL conducted initial testing to characterize cell behavior without the use of passive intumescent material. This was necessary to inform DNV GL's understanding of the cells' heat and gas generation rates, to support material design. Video and extensive thermal data were also collected. Secondary testing, incorporating the passive intumescent material and off-gas sensors, was also performed. DNV GL compared results from the single-cell tests performed on 18650 cells with pouch cells used for Maritime applications, where data indicated that the 18650 cells were intense in their failure mode due to constrained construction and high energy density with short duration fires and high peak temperature per kg. During the initial tests, DNV GL tested the performance of Nexceris' Li-ion Tamer sensor for early detection of cell off-gas release, assessing how it may be used to prevent or limit thermal runaway of lithium ion (Li-ion) cells. Additionally, DNV GL described challenges faced during preliminary cell failure testing,

lessons learned thereof, and recommendations for future testing. The preliminary testing data was also used to inform the modeling approach for the prototype battery pack design.

Third, DNV GL collaborated with Thornton Tomasetti to perform flow and thermal modeling for battery thermal management and venting of gases released from cells under thermal failure conditions. The modeling work utilized a two-part approach, wherein initial modeling leveraged a 1-dimensional (1D) method, with more detailed computational fluid dynamics (CFD) modeling employed during final analysis. The initial 1D modelling demonstrated theoretical steady state venting, which provided exhaust duct constraints. The second part of the modeling exercise focused on transient venting analysis with heat transfer and exhaust restriction.

Fourth, and finally, DNV GL performed the final round of tests on the constructed prototype, including all the mitigative design features and cells within the designed battery module. In the tests, DNV GL initiated thermal runaway in a cell placed in the prototype module constructed of an intumescent block from Pyrophobic, and paired with the Li-ion Tamer early detection sensor. This qualification testing also enabled verification of thermal runaway cascading protections and heat dissipation. Based on the testing performed on the prototype battery module, DNV GL created acceptance criteria and templates for the CAB to outline the appropriate methodology by which compliance with design standards could be confirmed for the advanced battery module system. Five test procedures and results templates were outlined to assess criteria central to a design's acceptance: thermal runaway or failure, cascading thermal runaway or failure protections, containment of failure, reduction of failure impact, and monitoring. Based on these same criteria, DNV GL prepared design package requirements for the CAB to outline the central design objectives for this prototype, allowing future adoption of this design with identical or alternative suppliers and equipment. As a final task, DNV GL contextualized the battery module prototype within the evolving standards environment and assessed innovative applications for the design, such as urban air mobility.

1 Introduction

1.1 Battery system safety state of the art review

General hazards that threaten all electrochemical energy storage devices can be categorized by mechanical, electrical, and thermal abuse mechanisms. These abuse factors can lead to physical damage, emission of flammable gasses, thermal runaway, and cascading thermal runaway. In the event of an electrochemical storage device fire, all such hazards need to be fully managed and mitigated in order to deem the fire extinguished. Figure 1 provides a general overview of the abuse mechanisms and consequences.

A review of the lithium ion (Li-ion) incident history indicated that common failure modes are as follows: overcharge, external short, high temperature, and external impact. In nearly all cases, the stimulating event was external. In addition to being external, a lack of cascading protection between the cells allowed the event to become much worse, and in many cases failure to separate the cells in any way allowed the fire to become exponentially worse. In some cases where no cascading protection exists, the battery cells may melt or merge into an even larger mass, further exacerbating the fire threat.

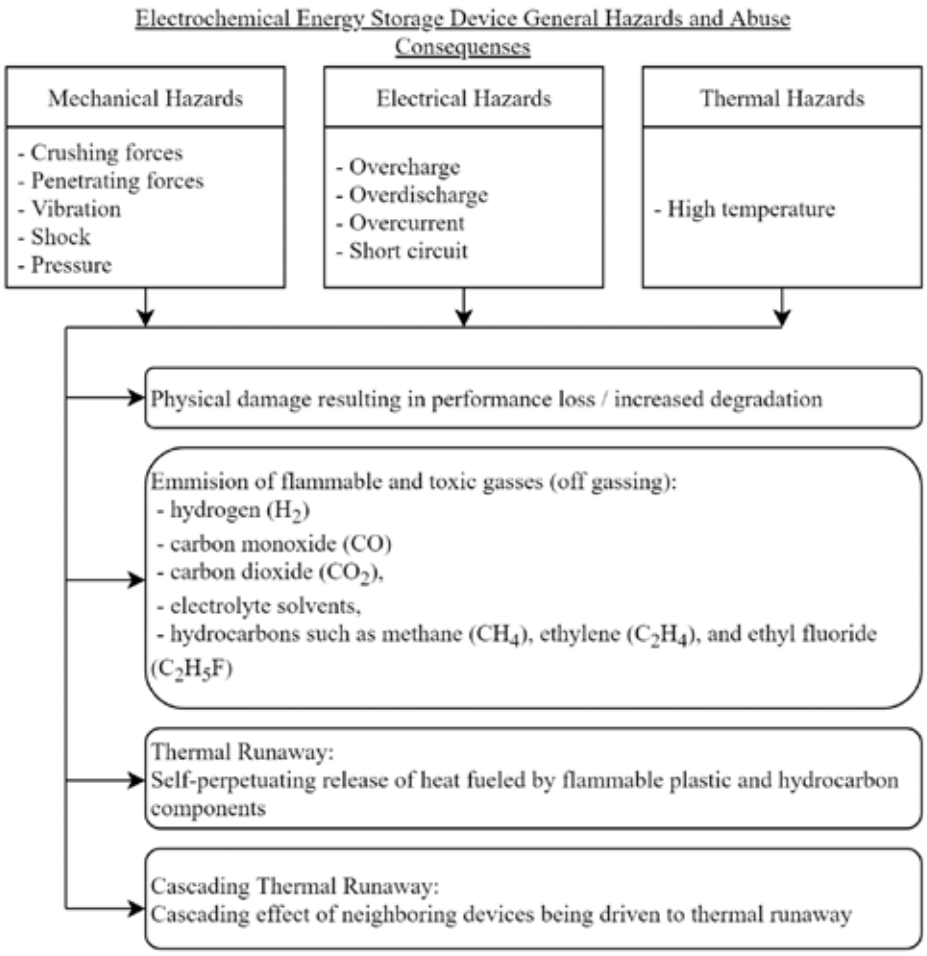

Figure 1. Electrochemical hazards and consequence overview

Energy and power are important from a safety standpoint. The greater the energy contained in the electrochemical device, the greater the damage potential if the energy is released rapidly through a failure or other abuse event.

General battery performance ranges and limits also impact safety. All batteries have an ideal temperature range. High temperatures (generally above 30 °C – 40 °C) tend to degrade capacity severely. Charging at high temperatures poses a safety risk and charging at high currents at very low temperatures (near 0 °C) can also present a safety risk for some Li-ion batteries. Other battery performance parameters such as c-rate, which relates to cell currents, and state of charge (SOC) and depth of discharge (DOD), which relate to cell voltages, also impact battery degradation. Depending on the battery chemistry, each of these parameters can contribute to safety risk. Temperature alone, such as exposure to fire, can induce battery failure. A high SOC or actively overcharged condition, in addition to temperature, can also create a safety risk. High

c-rates, especially at elevated temperatures, pose safety risks due to internal heating during discharge as well as the potential for separator breakdown and a short.

The battery fire hazard is not unlike the same hazard that exists for fuel. High temperature, flame, spark, crush, or puncture can lead to fuel fires. One must take the same precautions to avoid such hazards with battery systems. Numerous codes and standards currently exist or are under development for energy storage technologies, operating in a range of applications. Of prime interest when determining the minimum standards of safety at the cell and module level are UN 38.3, UL 1642, UL 1973 and IEC 62619. These standards include tests that focus on ensuring that the battery is resilient to typical dangers associated with shipping, to their use in consumer devices, and to the abuse they may face when installed in the field. In the stationary energy storage space, fire safety related codes are continuously developed and published by organizations such as Underwriters Laboratories (UL) and the National Fire Protection Agency (NFPA); notable standards include UL 9540 and NFPA 855.

In the aerospace and aviation sector, DNV GL has identified two standards from the Radio Technical Commission for Aeronautics (RTCA) geared toward the safe design, implementation, installation, operation, and maintenance of lithium ion batteries:

- RTCA DO-311 Minimum Operational Performance Standards for Rechargeable Lithium Battery Systems
- RTCA DO-347 Certification Test Guidance for Small and Medium Rechargeable Lithium Batteries and Battery Systems.

RTCA DO-311 lays out the minimal operational performance standards for rechargeable Li-ion batteries, whereas RTCA DO-347 details the testing procedures for small and medium rechargeable Li-ion batteries. These aviation standards are far more comprehensive than land-based stationary storage, as would be expected given the requirements for safety in such a setting. To that end, the RTCA 311 contains 33 tests for performance, electrical safety, and thermal safety. While the other previously described standards lay out no performance requirements, RTCA standards layout stringent performance requirements. From an environmental and safety perspective, the standard includes 11 environmental or mechanical tests and with a far wider range of threats than stationary applications, including such concerns as fungus resistance. Finally, this standard outlines more specific requirements for attached power electronics, including significant reference to additional RTCA standards.

RTCA DO-347 covers far smaller batteries and small systems, which, while comparable to UL 1642 or IEC 62619, are much more thorough and stringent with regards to passing criteria and

performance requirements. Additional safety testing standards that examine the volatility or stability of battery cells and modules include IEC 62281, NAVSEA S9310-AQ-SAF-010, UL 2580, and RTCA DO-347.

It has long been held within the energy storage industry that batteries are able to reignite anywhere from one minute to three weeks after initial thermal activity. The cause is a result of external stimuli on the damaged, and less stable, cells. This may occur as a result of electrical, mechanical, or, more commonly, thermal stimuli. In the case of thermal stimuli, the deep-seated nature of the fire makes it such that the residual heat within the cells is capable of reigniting the gases the battery is generating. At a cell level, testing of just two cells laid together showed that temperatures between the two stayed above 500 °C for up to 30 minutes after the initial failure. This is above the autoignition temperature of H_2. (This is important because DNV GL has observed gas generation from the cells for up to hours after the event so long as the material remains hot.) This prompts numerous considerations for first responders during overhaul and post fire operations, as well as handling of the cells after the event. DNV GL recommends against fire services handling the batteries after the event and strongly recommends against the use of piercing irons and nozzles when fighting battery fires. DNV GL strongly recommends adequate cascading protection be employed in systems to manage failures and prevent this behavior. DNV GL also strongly recommends that first responders continue to wear self-contained breathing apparatus or respirators even during overhaul and that they maintain awareness of ventilation and monitor gas levels in areas containing batteries.

1.2 CAB design philosophy established

This project investigates the effectiveness of a combination of technologies to mitigate Li-ion safety risks. To this end, DNV GL aims to develop a Li-ion battery pack comprised of 18650 cylindrical cells encased in an intumescent material, a special type of composite thermoplastic resin material that increases in volume when exposed to thermal energy, and an off-gas monitoring technology. Such a battery pack is expected to be able to better withstand thermal runaway; in part, by shutting itself off before thermal runaway can begin in earnest. Should this action fail to prevent cell fire, the intumescent material will envelop the failing cell, contain any conductive heat transfer and isolate off-gases, while a specially designed exhaust plenum will shuttle the gas away from the pack and to a safe exhaust point. The technologies utilized in the project are as follows:

- Pyrophobic® Lithium Prevent® - A passive thermal containment technology from Pyrophobic Systems, LLC that mitigates cascading thermal runaway and contains a high energy release.
- Nexceris® Li-ion Tamer® - Off-gas monitoring technology designed to provide advanced diagnostic feedback for Li-ion battery systems.

The battery pack design was based on specifications provided by General Atomics for their unmanned aerial products. Consequently, a 7S-5P setup, or 35 total cells, was used to meet the performance specifications laid out for the battery pack; 5 parallel strings, each with 7 series connected cells. A block of the Pyrophobic material was used, with a honeycomb like lattice cut out for the cells. As part of the design strategy, DNV GL proposed to quantify the thermodynamic and fluid dynamic behavior of battery off-gas. This data was expected to be used to optimize the exhaust plenums fitted to each cell or cell group, and the Nexceris sensor's placement at the most opportune point within the exhaust plenum to detect early gas emission prior to failure. Thornton Tomasetti's Weidlinger Applied Science (TTWAS) group conducted computational fluid dynamics modelling of gas flow. This modelling was expected to guide the shape, diameters, and angles of the exhaust plenums and manifolds required.

1.3 "Drop-in" battery solution design criteria

DNV GL created design criteria for a battery solution design to fit within existing systems. The battery pack design criteria included physical dimensions of the pack, series-parallel configuration of the cells and their arrangement within the pack, thermal and ventilation management within the pack, the battery management system (BMS) that controls cells voltages and currents and prevents electrical abuse, and integration of the intumescent material and off-gas monitoring technologies. The tables provided in Appendix A can be utilized as checklists for criteria that are necessary to make a new battery solution design fit within existing systems.

1.4 Materials and cost list, BMS functions

This section describes the implementation of Nexceris' off-gas monitor into a BMS as well as an estimate of materials and costs for the Commercial Advisory Board (CAB).

The Nexceris Li-ion Tamer off-gas monitor (OGM) has been designed for system integration through multiple device platforms. This device can be through-wall mounted into a battery enclosure or secured to a surface using a mounting bracket. The OGM can be powered through an optional connector or hardwired to provide the device with a supply voltage, while the signal return can be integrated into a system level controller, such as a BMS. The functionality of the

gas detection within the packaged OGM is located on a single circuit board that is wired into the packaged device. The device platform has been found to be suitable for multiple testing and system integration applications due to the non-invasive requirements for integration.

The OGM allows for detection of a single cell failure in parallel groups on cells without thermocouples and other abuse conditions that lead to off-gassing. Such early detection and consequent mitigating action can be used to electrically isolate the battery at the onset of gas detection, and may save the battery by stopping heat production via Ohmic heating or electrochemical processes. While it will not stop a cell that has fully gone into thermal runaway, and thus has begun consuming itself exothermically, this early detection may prevent the battery from reaching this state. This may also provide a back-up detection method in the case of BMS failure or inability to detect venting.

Material requirements for the OGM are based on the number of sealed modules in the battery system. A minimum of one daughterboard would need to be installed within each sealed module to provide monitoring of the gas space around the cells. At high volumes, the daughterboards could be provided on tape and reel packaging in compliance with Energy Information Administration (EIA) Standard 481 for automated handling of surface mount components. Table 1 below provides estimates of the material costs based on estimated annual usage numbers.

Table 1. Estimate of OGM daughterboard costs

Estimated annual usage (EAU)	**Estimated cost for OGM daughterboard**
100	$65
1,000	$35
10,000	$25

1.5 Functional requirements for adaptation

A punchlist of battery design criteria may consider the following requirements for adapting an existing system to new system designs. Table 2 shows a punchlist with actions for the CAB for each criterion.

Table 2. Functional requirements punchlist for battery system design

Draft Punchlist	CAB Actions
Exterior dimensions of battery module	Selection of location on aircraft.
Containment	Whether active pressurization is needed (depends on battery type) or if the battery system is located within a pressurized part of the aircraft.
Battery System weight	Weight savings may be realized with elimination of ancillary or supporting power systems.
Battery Module Voltage	This may be less relevant to the CAB than system Voltage.
Battery System Voltage	Considerations for connection to existing electrical infrastructure on aircraft.
Battery Module Current	This may be less relevant to the CAB than system current.
Battery System Current	Considerations for connection to existing electrical infrastructure on aircraft.
Maximum life considerations	Will be related to cost-benefit analysis.
Series-parallel configurations of cells (for optimum life and safety limits)	CAB should prescribe system voltage, current, cost. System integrator can determine S-P configuration.
Lowest cost considerations	CAB determines cost targets.
Cooling	CAB should consider availability or tolerance of closed loop cooling on the aircraft. Integrate with existing systems or stand-alone.
Required BMS criteria for system	
- cell specific voltage limits	Systems integration and design responsibility.
- cell specific current limits	Systems integration and design responsibility.
- cell specific temperature limits	Systems integration and design responsibility.
- error communication	CAB needs to specify who receives this information, where it is stored, who responds.
- BMS override of system commands	CAB repair procedures.
- "lock" of BMS which requires intervention and correction to override	CAB repair procedures.
Off-gas Monitoring integration into BMS	CAB needs to specify who receives this information, where it is stored, who responds.
Shutdown criteria from OGM to BMS	CAB needs to specify who receives this information, where it is stored, who responds.

Draft Punchlist	CAB Actions
Multi-functional intumescent material specifications	Depends on size and location specified by CAB.
- Intumescent material weight and dimensional constraints	Depends on weight criteria from CAB.
- Venting/gassing channels based on cell form factor	Direction from CAB on where to vent gases.
- Thickness of walls	Depends on weight, location, environmental criteria from CAB.

2 Basic cell block testing

2.1 0^{th} order design

During this phase of the study, DNV GL performed basic cell testing, which was conducted in two phases. Initial testing included characterization of the selected cells without the use of the passive intumescent material. This involved off-gas analysis via Fourier Transform Infrared Spectroscopy (FTIR) and potentially gas bag capture analysis (H_2 is a prevalent gas released, however, it is not detected by the FTIR). In addition, DNV GL used first principles to record heat release rate. This was necessary for understanding how the cells generate and release heat, which also assisted in material design. Video and extensive thermal data were also collected.

Secondary testing was performed incorporating the passive intumescent material and including the Nexceris OGM sensors. The goal of this stage of testing was to understand the difference in failure mechanics when the material is incorporated, to ensure it does not contribute to the gas generation in a way that will impact sensor analysis and to ensure that the material will work properly with whatever cell form factor is selected. This testing may also lead to additional tuning of the off-gas sensor.

Testing was performed in two types of chambers with the first being a large battery abuse testing chamber (LBAC) that DNV GL operates at the New York Battery & Energy Storage Technology (NY-BEST) Test and Commercialization Center in Rochester, New York. The second test setup consisted of a custom-built combustion chamber, with plumbed exhaust system and tubular manifold (TM), intended to determine gas release rates and exhaust requirements. The cells tested for this project were commercial off-the-shelf, Li-ion nickel manganese cobalt (NMC) cells in the 18650 format. The cells were shipped from General Atomics to DNV GL's NY-

BEST lab and were charged accordingly prior to each test. DNV GL provided additional 18650 cells, which were already available in the lab.

The LBAC has a volume of 0.44 m^3 and permits thermal, electrical, and physical abuse of Li-ion batteries in a controlled environment, such that the explosive and toxic hazards from battery fires can be measured and managed. The intent of the TM was to more properly simulate the intended end product: that being a tightly packed battery in a confined spaced with minimal volume beyond the vents and a narrow diameter plenum or duct to atmosphere. The intent of the TM then was to more adequately measure flow/release rate of the gas as well as understand the likelihood of combustion versus venting in a poorly ventilated space prone to oxygen depletion.

The tests conducted per this task, collectively called FAA Tests, used both radiative and conductive heat to cause cell failure in the LBAC and only conductive heat in the custom manifold chamber. The tests were conducted with a pre-test cell SOC of 100% and 50%. The test chamber fans were either turned off, triggered to activate with the Nexceris OGM sensor, or were active at 100% power during testing.

The test set-up included 13 thermocouples. Eight of these comprised a thermopile to capture convective heat release rate around the unit, two or three thermocouples were placed on the cells directly, and three thermocouples were placed in the chamber to measure ambient and inlet and exhaust temperatures. Thermocouples on the cells were placed on the top and bottom with the third thermocouple placed on points of interest, depending on expected thermal gradients.

Cell failure through external heating presents the primary mode of failure propagation once a single cell has failed. In DNV GL's experience as well, external heat exposure has proven to be the most reliable, and more importantly repeatable, method for creating cell failure. As such, all of the tests performed for this project focus on heat application. The FAA Tests included eleven separate tests. DNV GL conducted three types of tests, as follows:

- The first seven tests were performed in the LBAC without active ventilation. This was allowable, as the small size of the cells would not be expected to consume the entirety of the oxygen within the test chamber. Openings in the chamber would still allow air to draft in and out naturally. This would be similar to a semi-sealed volume, and once combustion began, oxygen levels would drop, as would be expected at altitude as well. Larger cells in this type of test would be expected to immediately consume all free oxygen in the chamber and go to a smoldering, low intensity flame until oxygen levels could be restored, typically via forced ventilation.

- The four subsequent tests performed in the custom tubular manifold chamber only used conductive heat to cause a failure. These tests allowed air flow, as ventilation was active, all holes in the bottom of the unit were left open, and some holes along the sides and top of the unit were left open. Based on previous DNV GL work, the density of the gas released varies depending on the properties of the combustion and ambient atmosphere. As DNV GL seeks to determine what additional ventilation rates may be required, this test sought to realistically simulate the setup.
- A third test method was conducted with a constrained pouch cell in the LBAC with active ventilation. The cell was constrained using metal plates to simulate the resistance of neighboring cells, while still allowing for some degree of swelling and deformation.

Additional DNV GL Maritime tests examined other failure modes besides external heat, such as overcharge and short circuit conditions. An overcharged cell can cause the electrolyte to decompose, generating flammable and toxic gasses with an increasing proportion of the energy input converted to heat due to increased cell impedance. Internal short circuits are caused by the formation of a conductive bridge between the positive and negative electrodes inside the battery cell. The majority of internal short circuits do not result in a thermal event. However, thermal events are possible if the impedance of the short circuit is high enough to create sufficient heat, but low enough to allow sufficient current to pass and the conductive bridge is strong enough to withstand current flow. External short-circuiting, as conducted here, may be indicative of an electrical failure or human factors where the circuit as a whole is shorted.

During each test, DNV GL examined the release of gases when batteries undergo thermal runaway. Gas data was collected by DNV GL's FTIR gas analyzer, a Gasmet DX4000. This unit sampled the chamber internal atmosphere at approximately every six seconds. In addition to the FTIR analyzer, MSA Ultima fixed gas sensors were used to validate the O_2 measurement, as well as monitor for H_2 and the overall lower explosive limit (LEL). The observed gases include water vapor (H_2O), Carbon dioxide (CO_2), Carbon monoxide (CO), Methane (CH_4), Ethane (C_2H_6), Ethylene (C_2H_4), Hydrogen chloride (HCl), Hydrogen fluoride (HF), Hydrogen cyanide (HCN), Benzene (C_6H_6), Toluene (C_7H_8), Ethanol (C_2H_6O), Methanol (CH_4O), and Oxygen (O_2). Peak gas concentrations observed between FAA and Maritime tests is shown below in Table 3.

Table 3. Peak gas concentrations according to FAA and Maritime tests failure modes

Gases Measured	Unit	FAA		Maritime		
		Radiative & conductive heat	Conductive heat (tubular chamber)	Radiative & conductive heat	Overcharge	Short circuit
Water vapor (H_2O)	%	4	4	4	4	4
Carbon dioxide (CO_2)	%	2	29	18	11	2
Carbon monoxide (CO)	ppm	9,205	299,759	51,777	237,099	12,639
Methane (CH_4)	ppm	327	185,818	173,638	221,233	2,143
Ethane (C_2H_6)	ppm	810	50,708	46,998	110,624	2,756
Ethylene (C_2H_4)	ppm	479	153,929	69,230	83,309	450
Hydrogen chloride (HCl)	ppm	27	58,447	74,215	15,240	83
Hydrogen fluoride (HF)	ppm	16	623	878	328	11
Hydrogen cyanide (HCN)	ppm	8	415	12	20	9
Benzene (C_6H_6)	ppm	1,540	3,405	5,687	2,744	1,453
Toluene (C_7H_8)	ppm	88	10,513	2,573	2,019	1,102
Ethanol (C_2H_6O)	ppm	153	36,904	74,710	36,341	6
Methanol (CH_4O)	ppm	47	1,599	7,744	13,236	255
Oxygen (O_2)*	%	9	0	0	0	10

Temperature characteristics observed during LBAC tests:

- Cell was overheated via radiative and conductive heat with an initial SOC of 100%, without active ventilation (fan off).
- Initially, a steady temperature rise in the cell was observed.
- While temperature continued to increase, a small temperature drop was observed, which could be attributed to the cell venting as gas generation from degrading electrolyte created pressure greater than the designed venting pressure. This behavior is shown in Figure 2 below. This gas release may serve to temporarily “cool” the battery, releasing hot gas that has absorbed a great deal of energy via phase change. This effect is short

lived, and the result of the loss of this gas (which was evaporated or boiled electrolyte) is a system drastically less capable of managing the heat that continues to enter.

- A rapid temperature rise was observed at one point on the cell, with temperatures exceeding 500 °C, indicating thermal runaway.
- DNV GL further adds that this temperature is in line with combustion temperatures observed during thermal runaway, which is less a homogenous event as the beginning of several possible outcomes involving combustion, explosion, or high-pressure release of gas. During combustion, temperatures may increase to as high as 750-850 °C, whereas during venting, temperatures tend not to exceed 350-400 °C.
- Temperatures continuously dropped during the remainder of the test.

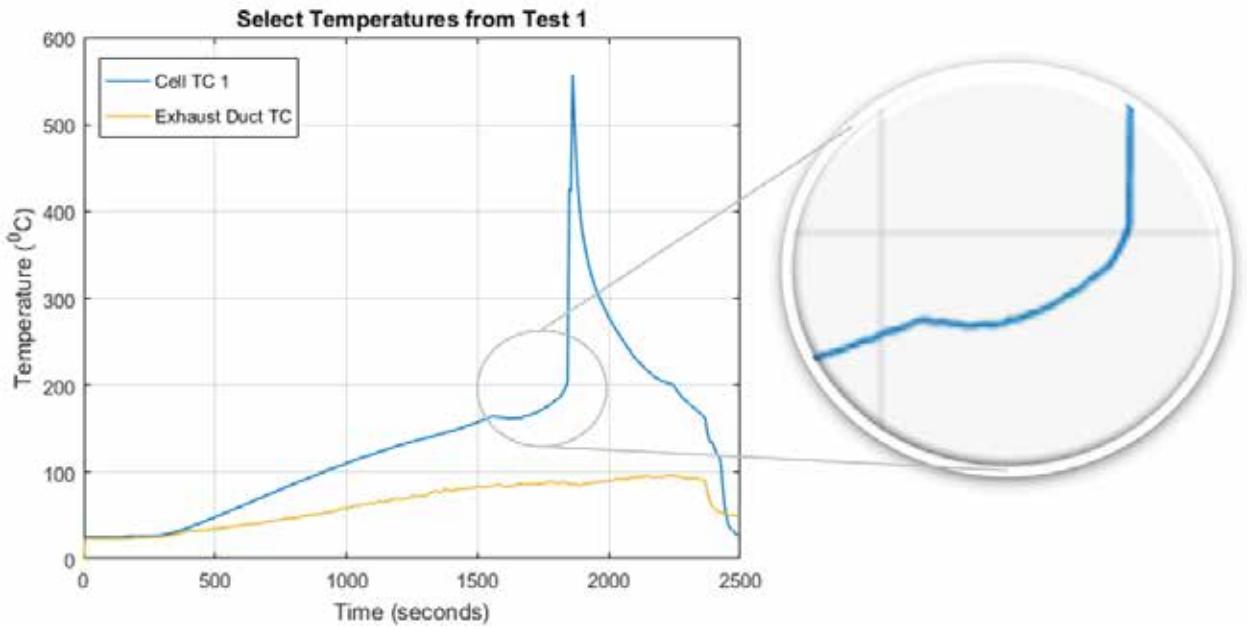

Figure 2. Example cell temperature behavior during test

Voltage characteristics observed during LBAC tests:

- Initially, cell voltage was seen to rise with rising temperature.
- Then cell voltage suddenly reversed polarity, which can be attributed to current interrupt devices (CID) installed in the 18650 cylindrical cells. The CID can open circuit the cell during failure, gas generation, or high heat.
- At this point, the CID is likely damaged or destroyed and the reliable voltage measurements cannot be obtained.

- This behavior is common in 18650 cells and shows that while the CID device may work as intended during single cell failure events involving overcharge, it should not be considered a reliable protection method when the cell is exposed to high temperature.

Numerous gas analyses were performed during the testing, primarily with DNV GL's FTIR gas analyzer; however, one fixed gas sensor separate from the FTIR provides a different picture of the gas release by looking at the overall explosivity, or percent of LEL, of the mixture of the gases. For the performed tests case, the mixture of gases in the chamber were typically less than 10% of the lower possible explosive concentration. However, this does not imply anything about the atmosphere locally surrounding the cell and suggests that a reduction in volume by a factor of 12, which would be in line with the volume of our expected design concept, would lead to an atmosphere that is indeed explosive. Coupled with the high temperatures (in excess of the auto-ignition temperature of hydrogen, which makes up much of the gas) and electrical nature of the design, the potential for ignition of this atmosphere exists should these gases not be rapidly removed from the system.

Gas release characteristics observed during LBAC tests are provided below:

- Gas release is initially observed toward the end of the steady temperature increase and just before thermal runaway.
- An uptick in explosivity is observed simultaneously with thermal runaway. This relates to a number of factors including the limitation of the sensing devices to detect gases, their temperature and concentration relative to Oxygen levels, and the complex makeup of the gases that keeps the initial release from being less flammable. Once thermal runaway occurs, the mixture rapidly becomes much more explosive, despite a further decrease in oxygen levels (oxygen levels impact explosiveness, with lower oxygen levels making atmospheric explosion less likely).
- At the initial venting event, measurable quantities of both CO and benzene are observed, as the breakdown of electrolyte and plastics (typically the separator and binder) in the cell is prone to generation of these gases. Lithium ion batteries tend to generate very large quantities of CO with nearly equal parts hydrogen (H_2), which cannot be detected by the FTIR but has been observed by gas capture in numerous past experiments.
- While a rapid increase in gases in the chamber is observed from initial venting, this event itself is not indicative of combustion, as temperature increase remains steady and stable and by products of combustion, in particular CO_2, are not observed. As the cell continues to heat between this initial venting and ultimate thermal runaway, the ventilation system succeeds in bringing oxygen back into the chamber until thermal runaway and

combustion. At this point, had other indicators, including visual signals, not suggested combustion, the presence of CO_2, a product of combustion but not of electrolyte decomposition, would suggest that combustion had finally occurred.

- Thereafter Benzene, Ethylene, Methane, and Ethane are released in lower quantities during the test but in line with the events observed throughout the thermal runaway process. Ethylene is one of the ester-chains of choice for most Li-ion battery electrolytes, which typically include ethylene carbonate, dimethyl carbonate, and others. The breakdown of these compounds results in ethylene and methanol, whose further breakdown results in ethane and methane. These gases are all highly flammable, and their flammable and explosive limits are much lower than CO, which is over 10%. These gases, which are generated as the electrolyte is evaporated or boiled, and ultimately decompose, are released during initial venting. However, once an ignition source, in this case combustion from thermal runaway, becomes present, their values decrease as they burn up. Once the fire begins to die out, concentrations of these gases again increase as a lack of oxygen does not sustain complete combustion, creating a fuel rich mixture, which may be reignited later, should inadequate ventilation fail to remove it and oxygen be reintroduced.
- Finally, discussion of corrosive and toxic gases generated during lithium ion battery failure is required. The observed gases include Hydrogen Chloride (HCl), Hydrogen fluoride (HF), and Hydrogen Cyanide (HCN). Observed concentrations of these gases were equivalent to burning plastic and other legacy technologies such as lead acid and nickel cadmium (NiCd) cells. However, these gases do still exist and in sufficient quantity may still create an atmosphere conducive to corrosion and necessitating an overhaul of sensitive electronics. DNV GL has also observed that a number of new cells and manufacturers are going to binder and coating materials rich in fluorine, with polyvinylidene fluoride (PVDF) plastic being particularly prevalent. This substance does tend to drastically increase the concentrations of HF observed, and while DNV GL's initial work suggesting that HF levels from the Lithium Hexafluorophosphate ($LiPF_6$) in the electrolyte creates far less HF than originally anticipated, the increasing prevalence of PVDF and other fluoridated plastics has drastically increased the presence of HF in some battery failures. Further, it bears mentioning that polyvinyl chloride (PVC) plastics, which are typically used for the wrappers of many cells, may emit HCl and CO during heat exposure but are not themselves indicative of failure, venting, or combustion.

An example of gas release from cell testing is provide in Figure 3 below.

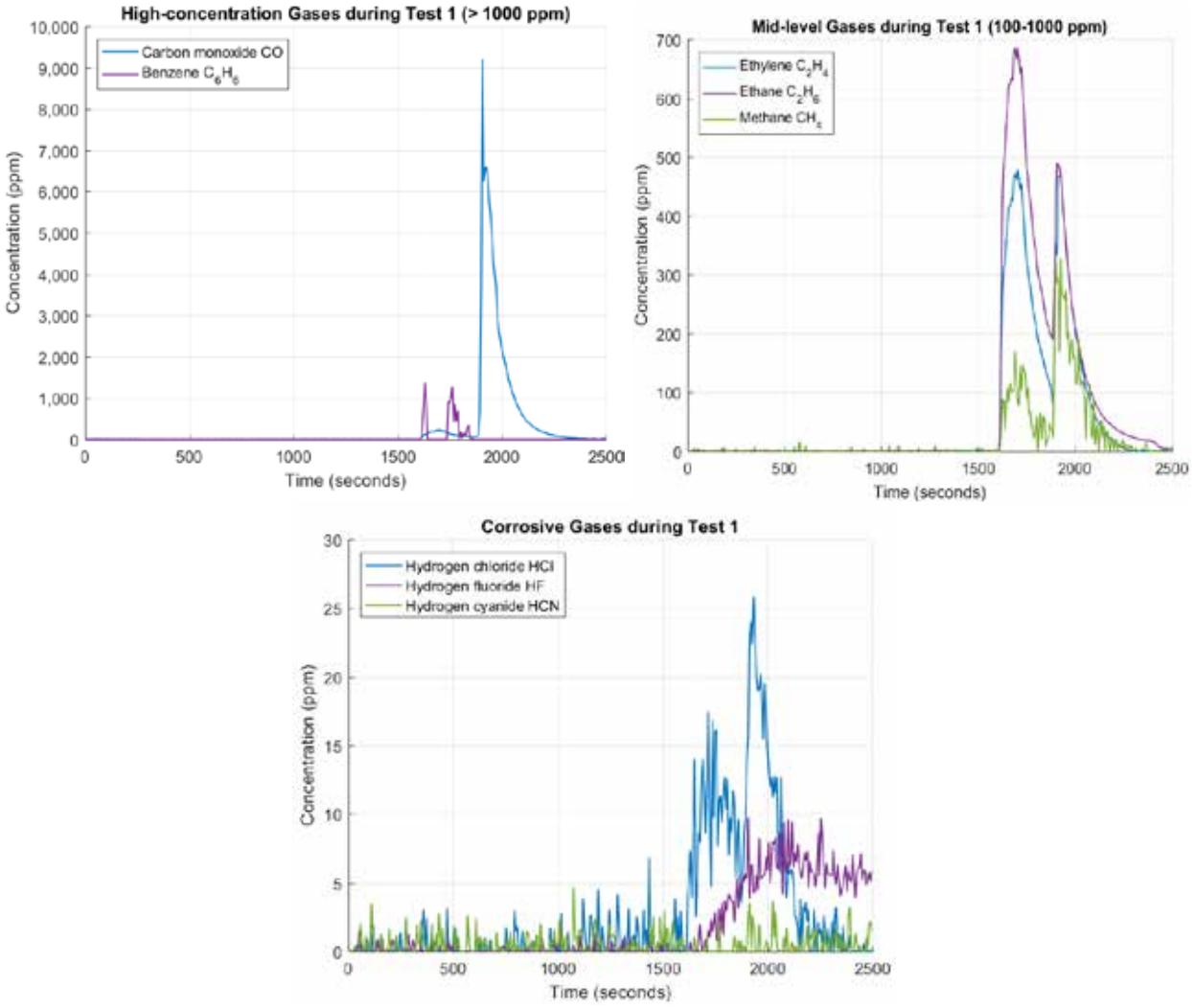

Figure 3. Example gas release from cell test (high-concentration gases, mid-level gases, and corrosive gases)

The TM tests displayed similar characteristics to the LBAC tests discussed above, with respect to temperature and gas release characteristics leading up to and during thermal runaway. A high-level summary of the characteristics observed during TM tests follows:

- As conductive heat is continuously applied through a film strip heater, with the fan on, battery cell temperature steadily rises to approximately 200 °C, slightly drops indicating initial venting, and then rapidly increases to above 500 °C, indicating thermal runaway. After this point, temperatures start to decline steadily through the end of the test.
- Gas releases indicate that thermal runaway had started and includes the byproducts of cell combustion.

- O_2 within the small volume of the TM is displaced quickly during the peak temperature event. The exothermic nature of the thermal runaway event is evident, regardless, and the temperatures above 250 °C are sustained for hundreds of seconds.

Overall test result characteristics:

- Temperature – Similar temperature characteristics were observed in all tests.
- Impact of pre-test SOC – The results displayed observable correlations with higher initial SOC resulting in higher cell temperatures, and higher initial SOC with higher mass loss.
- Gas release – Measured gas concentrations were higher in the TM compared to LBAC. This can be attributed to the smaller volume of the TM.

The TM tests also included a Nexceris OGM sensor, with some tests additionally including the intumescent material. For the tests without the intumescent material, the OGM sensor triggered well in advance, hundreds of seconds, of thermal runaway. For tests that included the intumescent material, the OGM sensor triggered concurrently with thermal runaway. The observed results indicate that the intumescent material block might have interfered with the Nexceris OGM sensor's ability to provide early detection. However, DNV GL cannot confirm this without further testing.

Some challenges encountered during the testing process are included below:

- Voltage measurement of 18650 cells without tabs proved to be challenging. The tabs were destroyed once the gas venting and thermal runaway process started, making it impossible to get reliable voltage measurements.
- Peak gas concentrations, especially in the smaller TM testing chamber, far exceed the calibrated range for the FTIR. For instance, the FTIR is calibrated to record CO up to 30,000 ppm; however, three of the four tests in the TM show peak values well above 200,000 ppm, though it is possible 20% of the air was CO; this measurement is far beyond the linear or reliable range of the device.
- In some cases, it was not possible to measure cell mass loss at the conclusion of a test due to the cell being lodged within the intumescent material blocks.

2.2 Heat loads and duration of events

This section compares results from FAA and Maritime tests, conducted on commercially available cells from 2017 to 2018, to prior testing performed by DNV GL on cells from 2015 to 2016. One of the main references includes a DNV GL study performed for Consolidated Edison

(Con Ed) and New York State Energy Research & Development Authority (NYSERDA) that provided considerations for fire safety for various battery chemistries[1].

Compared to cell and module burn testing conducted in 2016, the FAA and Maritime tests demonstrated higher energy density and shorter duration burns than previously studied, as shown in Figure 4. The duration of events, including the majority of mass loss and gas emissions, ranges from 2 to 17 minutes across the cells tested in this program, whereas the previous tests took between 20 and 65 minutes. Although some data collection challenges were encountered, as described below.

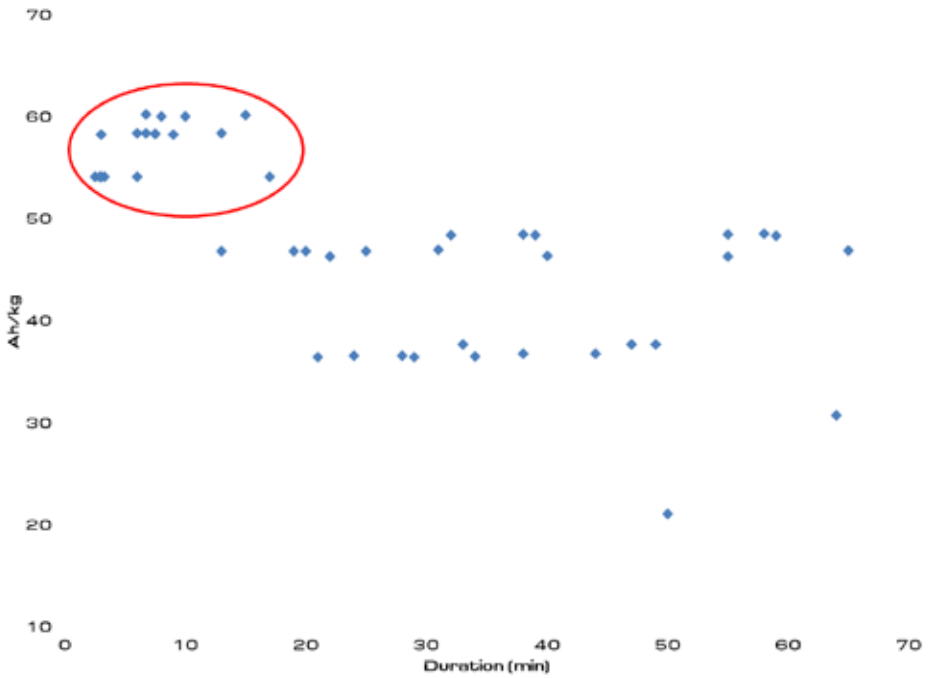

Figure 4. Results of FAA testing (circled in red) compared to cell safety testing in the Con Ed program from 2016

Peak temperatures for the present testing are comparable with what has been observed in prior testing. This result is as expected, as battery cell construction materials have not changed the fuel of the fire to a substantial degree, only their density. Both new and old data indicated an inverse relationship between cell physical size and peak temperature. That is, smaller cells displayed a

[1] DNV GL. Considerations for ESS Fire Safety. February 9, 2017. Accessible here: https://www.dnvgl.com/publications/considerations-for-energy-storage-systems-fire-safety-89415

higher peak temperature per Ah. The 18650 cells were intense in their failure mode due to their constrained construction and high energy density, with short duration fires and high peak temperature per kg.

Some challenges encountered during tests include the following:

- In FAA Test 4, the thermocouple was destroyed through deflagration of the cell and temperatures were only recorded prior to that point.
- In FAA Test 6, an explosion forced the cell onto the band heater and caused a short, resulting in data collection errors.
- In DNV GL's Maritime Test 7, the mechanical contactor used during this short circuit test overheated and was destroyed. The contactor was believed to handle a couple thousand amps, though the test revealed this not to be true.

2.3 Demonstrated early warning

During initial testing, DNV GL heated cells well beyond normal operating conditions[2]. While heat was applied externally, the intent of the tests was to simulate internal heat generation from an internal defect. While this test exposes the cell to more heat than it may reasonable generate, it does allow the electrolyte inside to be gasified or vaporized as it would, and creates separator failure that leads to thermal runaway. As a result of this gas generation, the cell will ultimately release gas through a designed pressure release valve or vent which opens at a predetermined pressure. While this vent typically blows open violently during catastrophic failure, the vent may crack or the seals on the vent may begin to fail slightly because of high temperatures. This allows trace amounts of gas to escape seconds to minutes before the cell fails completely. It is at this point that the Nexceris Li-ion Tamer sensor may detect gas released from the cell and potentially isolate or shut down the system. Li-ion Tamer is a relatively simple volatile organic compound (VOC) sensor that is specifically tuned to the VOCs used as battery electrolyte. The sensor also has a special ramp rate algorithm imbedded into it such that regular, slow leakage from the cell does not generate a false positive signal. In some cases, the ensuing shutdown may be done promptly enough to prevent the failure from advancing to a catastrophic event.

In many cases, the value of the Nexceris sensor comes when a single cell fails within a parallel cell group or when a cell fails that is not monitored by a thermocouple. These failures may result in gas release, which can be detected by a single sensor for the entire pack, and allows for a

[2] Short circuit and overcharge tests were also performed, and results discussed, but most tests examined failure through heat exposure.

reduced data acquisition requirement since single cell failure may be detected by a single sensor. As has been seen in failures investigated by DNV GL, sensor failure or an under-monitored pack allows errors and unsafe conditions to exist and exacerbate. Many cell failures can result in an electrical failure that does not provide a voltage indication, especially when grouped in parallel with other cells. These factors then result in a need for failure detection when comprehensive temperature data is not available. An example of early warning detection can be seen in Figure 5 below.

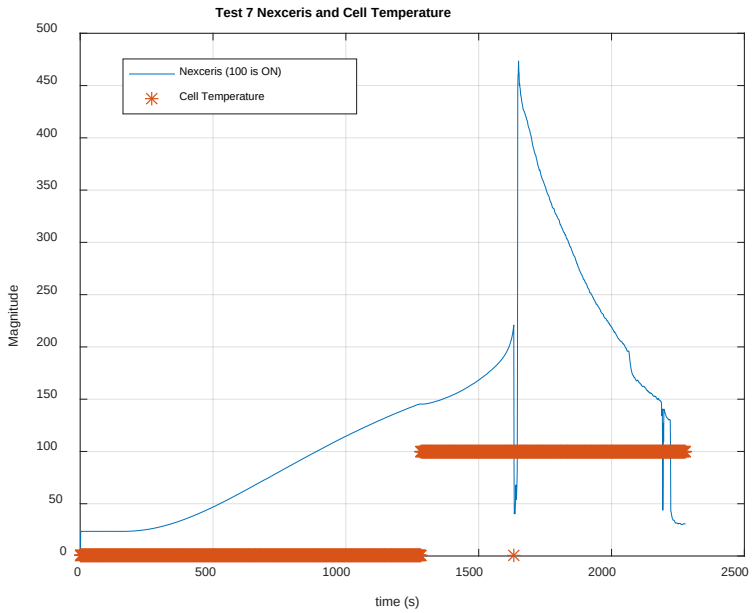

Figure 5. Nexceris early warning detection and cell temperature

Summary of key findings:

- FAA Test 7: Conducted in the LBAC with fan off. The Nexceris Li-ion Tamer OGM sensor detected gas release, indicating cell failure, and triggered several hundred seconds before thermal runaway.
- FAA Test 8: Conducted in the TM with fan on but restricted air flow. The OGM sensor triggered almost 90 seconds before thermal runaway. The TM is of considerably smaller volume than the LBAC and replicates a confined space. The Nexceris sensor successfully provided early warning in this confined space. Within minimal air flow through the device, the sensor, which was placed approximately 18” downstream and 10” above the

chamber in vertical direction, managed to detect thermal runaway several tens of seconds prior to thermal runaway occurring.

- FAA Test 9: Conducted in the TM with fan on but restricted air flow. Nexceris sensor detected cell failure several seconds before thermal runaway. In this case, air flow through the TM was even more restricted, as the inlet solenoid remained closed, effectively reducing airflow to nearly zero. Despite this, diffusion of the off-gas through the system was still detected by the sensor. The Nexceris sensor also detected off-gas before the FTIR detected carbon monoxide, albeit the FTIR inlet was located several inches higher up the TM plenum.
- FAA Test 10 and FAA Test 11 did not provide early detection of thermal runaway. Instead, the OGM sensor triggered concurrently with thermal runaway.
- Maritime Testing – External Heat Exposure: External heat was applied at the top of the cell only. As a result, the temperature at the time at which the Nexceris sensor activated was below the 65 °C, which is the Radio Technical Commission for Aeronautics (RTCA) standard high temperature threshold for failure. The OGM sensor detected failure hundred seconds before thermal runaway.
- Maritime Testing – External Short Circuit: The short circuit test, as intended was not successful. Cell temperatures remained between 20 °C and 25 °C during the test. The short circuit current exceeded the expected 3,000 A range and the mechanical contactor with the cell failed catastrophically. The Li-ion Tamer detected off-gas from the failing cell approximately 75 seconds after the short circuit.
- Maritime Testing – Overcharge to Failure: The Li-ion Tamer sensor detected cell failure hundreds of seconds prior to thermal runaway and tens or hundreds of seconds before a high temperature warning would have detected issues. The OGM sensor detected failure at cell temperature below 50 °C, below the RTCA threshold of 65 °C and possibly safety alarms.
- Maritime Testing – Overcharge to Shut Off: This test demonstrated definitively that using the Li-ion Tamer sensor to disconnect a failing system can prevent battery failure from turning into thermal runaway. During this test, the cell was charged at 50 A (0.8 C) but current was disconnected once the sensor activated. Upon disconnection, the battery temperature and voltage stabilized, and the cell remained stable for over two hours until DNV GL applied heat to the cell to neutralize it.

Some challenges encountered during cell failure testing are described below:

- Maritime Testing – External Short Circuit: The short circuit test, as it was intended, failed. An electromechanical contactor was used in the test to close the circuit, with 4/0

wire used to connect the battery to the contactor. In addition, a discharge current of approximately 3,000 A was expected, which was within the contactor's one-time rating of 10,000 A. Though current was not measured, it is believed to have exceeded the expected 3,000 A, as the mechanical contactor failed catastrophically, exploding in the chamber. The wire carrying the current also failed, with its insulation bursting into flames. This event proved more severe than the battery failure, which itself was merely a venting of the cell and mild candle flame.

2.4 All demonstrated binary off-gas triggers for shutdown

This section describes binary off-gas triggers demonstrated by the Nexceris OGM device, and how it can be used to mitigate thermal runaway of Li-ion cells. The Nexceris OGM provides a binary detection output via an analog output signal. The OGM outputs three diagnostic states: No power to device – 0.00 Vdc, Gas sensor signal out-of-range – 0.10 Vdc, and Start-up Condition – 0.25 Vdc. The binary outputs during normal operation are: Ready – 0.50 Vdc, and Off-gas Detected – 3.00 Vdc. A gas sensor provides a continuous raw output proportional to the amount of gas detected by the sensor. This continuous output is fed into an event detection algorithm, which interprets the signal to provide a discrete (binary) output that indicates when a cell has vented based on the gas sensor output signature. The binary output from the OGM can then be used to signal shutdown of a battery to mitigate the risk of thermal runaway. DNV GL verified this functionality through thermal abuse tests performed on 18650 cells.

In the first test, the off-gas detector was used to monitor the cell for off-gas while the cell was thermally abused until it entered thermal runaway. This demonstrated the primary function of the output, which provided the on/off indication of off-gas when the cell vented 4.5 minutes prior to thermal runaway. When the OGM output was used to trigger the shutdown of the test, the thermal runaway was prevented by removing the abuse condition. These response characteristics were also observed and discussed in the FAA and Maritime tests in previous sections.

In the event that the signal from the gas sensor is not usable within the event detection algorithm, the output will read 0.10 Vdc to indicate that the off-gas monitor is not functioning. This error state would account for severe drift within the gas sensor signal, as well as loss of signal events such as loss of heating on the sensor element. Beyond these diagnostic states, the output from the off-gas detector is designed to operate in a binary manner; with 0.5 Vdc under normal operation and 3.0 Vdc once triggered.

The output of the OGM can be incorporated into a decision process for failure prevention or battery system health. A BMS typically monitors voltage, temperature, and current of the battery

pack. While it provides insightful and necessary data, it cannot detect single cell failure in parallel groups on cells without thermocouples. If the BMS fails, it may bring about the abuse conditions needed to cause failure. Incorporating the OGM in addition to the BMS will add redundancy to the battery safety system.

In cases where a battery is flight critical, knowledge of imminent failure may not allow the battery to be taken out of service, but passive intumescent material can be used to protect adjacent cells while appropriate changes are made to battery use to try to avoid failure. In this case, the incipient fault detection provided by the off-gas monitor could be communicated to the crew and allow them to decide how to proceed with the flight operations. If the battery system comprises multiple battery packs, it could be possible for the crew to isolate the compromised pack if the flight critical system is able to operate on reduced power. This could help prevent a catastrophic loss of the battery system if the intumescent material is not able to contain thermal runaway to a single cell.

2.5 Testing revisions

This section describes challenges faced during preliminary cell failure testing, lessons learned therefrom, and recommendations for future testing. DNV GL discovered the following regarding the test set-up:

- The test set-up was designed to measure gas flow rates on the order of 10 – 100 m/s and pressures in the range of 0 – 15 psig. However, the actual flow rate from exhaust was on the order of 0-20 m/s, not much higher. This resulted in a pressure range far greater than could be practically measured on our equipment.
- Without an opening in the bottom of the TM to allow for makeup air to flow through, two things happened that restricted airflow through the test set-up:
  - The fan, unable to effectively pull a “vacuum” given the setup, did not produce a sufficient pressure drop to actually flow air.
  - Without makeup air to replace the consumed oxygen, combustion was limited to the self-oxidation occurring within the cathode’s metal oxides. This reduction in free oxygen for combustion results in drastically lower air temperatures inside the chamber, relative to what was seen in the LBAC with far greater air flow as combustion, and thus chemical energy release, is limited.
- A lack of oxygen flow into the TM resulted in a lack of sustained combustion; and ensuing lower temperature resulted in a lower energy (denser) vapor cloud that was more prone to lingering in the chamber than escaping as a result of high pressure. This resulted

in far greater decay times for gas concentrations in TM tests compared to the LBAC. This effect has been further demonstrated in large scale (>20 kWh) testing done by DNV GL, where battery off-gas without combustion tends to drop, or pool into lower elevations, and results in explosive concentrations at ground level. Whereas batteries that are fully involved with fire expel all gases upward.

Findings from preliminary testing resulted in changes to the approach for modeling the required pressure differential to remove gases, flammability of the mixture, and heat transfer of the gas. These findings were also used to influence changes in the test setup for the final round of testing, which should provide the desired results without the errors highlighted above.

For the final round of testing, DNV GL shall correct previous shortcomings with the initial setup, as explained below:

- Improved Makeup Air Process – During initial testing, DNV GL used a single, small, electrically powered solenoid to allow airflow into and out of the tubular manifold setup. This device failed after two tests and may not have worked reliably during those tests. To this end, DNV GL shall acquire an explosion rated unit to replace the original, which shall be appropriately sized and placed further upstream from the test chamber, ideally reducing any impulse pressure exposure. DNV GL may also seek to use additional techniques for controlling air flow and back pressure, including check valves and air pumps or fans providing positive pressure versus the previous negative pressure technique.
- Improved Flow Rate Measurements – In previous testing, DNV GL attempted to use a pair of gauge pressure transducers rated for 0-15 psig. Even with 16-bit resolution on the data acquisition, the actual pressure differential observed between static and stagnation pressure for the actual flow rates did not exceed the noise and uncertainty of the measurement, thereby rendering the measurement worthless. DNV GL has remedied this on large scale testing by acquiring appropriately rated differential pressure gauges on the order of 0-200 Pa, which allows for measurements of flow rates in the 0-25 m/s range. DNV GL will also improve this measurements reliability by ensuring an adequate ratio of air to exhaust gases, which would drastically alter the density and skew the measurement per simple Bernoulli’s equations.
- Hydrogen Monitoring – Previously, DNV GL was using a 0-1000 ppm H_2 sensor from MSA. DNV GL has replaced this with an H2scan Hy-Optima 720B sensor, which can measure up to 5% hydrogen by volume.

- Improved Fan Placement – DNV GL will change air handling to allow for control of makeup air. Given the setup requirements, it may prove more practical to only run positive pressure. However, this is also likely to result in increased oxygen for combustion, which may impact heat release results among other factors. Should negative pressure be required, DNV GL will develop a new fan system such that it would simulate a negative pressure ventilation system in the deployment.

During initial testing, DNV GL sought to quantify the actual volumetric release rate and total gas release from a failing cell. This has frequently been cited, without sufficient data, to be approximately 2 liters/Ah. To accomplish this, DNV GL created the tubular manifold (TM) with the intent of creating a test setup more in line with the design concept, and where gas flow could be better measured and controlled.

To measure this volumetric release rate, DNV GL sought to measure the airspeed and temperature of gas moving through the tube. With temperature, and thus density, as well as a known cross-sectional area and velocity, DNV GL could then calculate volumetric and mass release rates including total heat release rate. To measure velocity, DNV GL sought to build a robust "pitot tube" like setup, where digital pressure transducers would take the place of a manometer to determine pressure differential. As DNV GL knew the hydrogen explosion that sometimes occurs during these failures could exceed several tens of pounds per square inch (psi), DNV GL wanted to ensure that this pressure wave could also be recorded. As such, DNV GL used 0-15 psi digital pressure transducers to capture static and dynamic air pressures through the tube, as shown below in Figure 6.

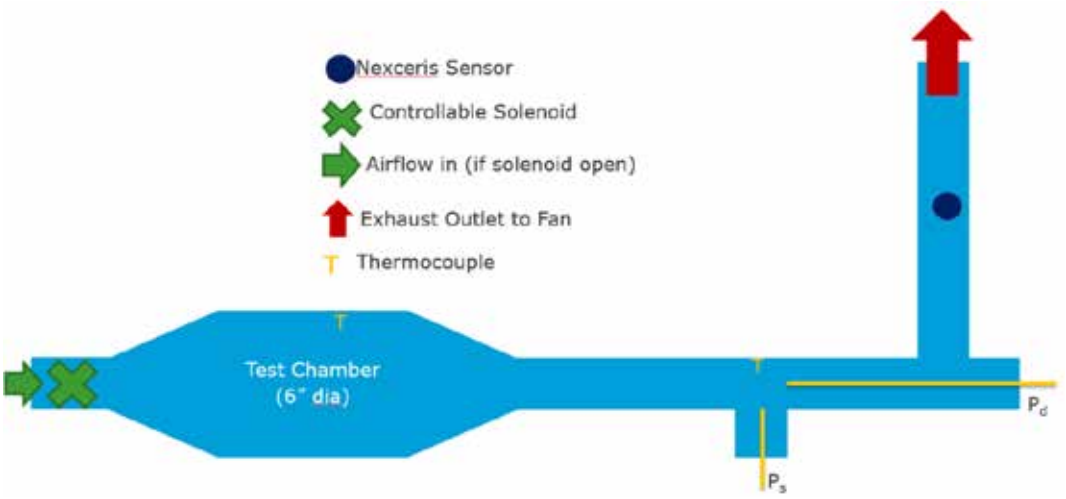

Figure 6. Tubular manifold test setup

Based on Bernoulli's equation, this would allow DNV GL to measure flow rates on the order of 10-100 m/s as well, which DNV GL believed to be reasonable. However, this proved to be incorrect for several reasons.

DNV GL discovered several anecdotal facts that have influenced both the conceptual design as well as the approach to modelling. These facts include:

- The actual flow rate from exhaust is on the order of 0-20 m/s, not much higher. This resulted in a pressure range far greater than could be practically measured on our equipment.
- Without an opening in the bottom of the TM to allow for makeup air to flow through, two things happen that restrict airflow through the test setup:
  - One, the fan, unable to effectively pull a "vacuum" given the setup, does not produce a sufficient pressure drop to actually flow air.
  - The other, far more interesting aspect was that without makeup air to replace the consumed oxygen, combustion is limited to the self-oxidation occurring within the cathode's metal oxides. This reduction in free oxygen for combustion results in drastically lower air temperatures inside the chamber, relative to what was seen in the LBAC with far greater air flow as combustion, and thus chemical energy release is limited.

During at least two tests, one can see "cyclical" response where oxygen levels drop in the chamber, then slowly rise as oxygen seeps back in until they again hit a level critical for combustion (~16%), at which point a rapid combustion/oxidation event occurs again, though with sufficiently low energy to effectively raise temperatures. This lack of sustained combustion and ensuing lower temperature resulted in a lower energy (denser) vapor cloud that was more prone to lingering in the chamber than escaping as a result of high pressure (from temperature). This was demonstrated in far greater decay times for gas concentrations in TM tests. This effect has been further demonstrated in large scale (>20 kWh) testing done by DNV GL where battery off-gas without combustion tends to drop, or pool into lower elevations, and result in explosive concentrations at ground level. Whereas batteries that are fully involved with fire expel all gases upward.

Additionally, and tangentially related to the discussion above, Bernoulli's equations also do not lend themselves well to gases of unknown density and the ratio of battery off-gas to makeup air should be as low as possible to ensure the density approximation is reliable enough to provide dependable results.

These findings resulted in changes to the modeling approach that will look at required pressure differential to remove gases, flammability of the mixture, and heat transfer of the gas. Additionally, these findings will influence changes in the test setup for the final round of testing, which should provide the desired results without the errors highlighted above.

2.6 Final parameters for modeling

Per the key findings of the preliminary testing, DNV GL changed the scope of modeling from finite element analysis of conductive heat transfer through the Pyrophobic intumescent material to computational fluid dynamics analysis of the gas release and escape. This approach focused on choking of the flow, that is the flow creating back pressure back into the manifold, and on 1D convective heat transfer into the Pyrophobic block. CFD analysis is expected to identify the requirements for ventilation and thickness of a Pyrophobic cover to minimize heat transfer into the unit.

3 Modeling

3.1 CFD models to modify cell block

This section describes the modeling work that DNV GL has pursued in collaboration with Thornton Tomasetti (TTWAS). The CFD modeling was focused on flow and thermal modeling for battery thermal management and venting of gases released from cells under thermal failure conditions. The modeling work utilized a two-part approach where initial modeling is performed through a 1D method, with more detailed CFD modeling being employed during final analysis. CFD modeling is computationally intensive and provides a lot of detailed information for the flow and thermal performance. Given that the vent design was not fixed, it was more efficient to determine the general characteristics of the release and vent performance by analyzing the general shape as a 1D optimization problem. This 1D approach can assess venting rate, bulk velocities, and bulk temperatures for a wide range of variables, including the following: altitude (gauge air pressure for pressure delta from the plenum); operating temperature; number of battery cells producing off-gas; amount and flowrate of off-gas per cell; exhaust manifold configuration; and makeup air. Detailed 3-dimensional (3D) analysis through a CFD tool, ANSYS CFX, was performed after the 1D analysis.

TTWAS 1D modeling and analysis was performed using a scenario where one failed battery was placed adjacent to two cells. The components that comprise the battery pack included the following: battery cells, intumescent layer, block, manifold cover, and exhaust duct. The mass flow rate was observed above each failed cell and the temperature at the interfacial boundary of

the cell and the intumescent material was considered the key output; heat transfer back into the failed batteries was not modeled. Initial conditions for the model include a temperature of 60 °C and a gas flowrate of 0 kg/s. An additional input to the model was the volume and composition of unignited gas release, which was based on results from DNV GL's initial cell testing (30% Hydrogen, 30% Carbon monoxide, 20% Carbon dioxide, 10% Methane, and 10% Ethylene).

In the 1D model (see Figure 7), heat was assumed to enter the domain as gas is released from cells. Most of the heat flow was assumed to be lost through the exhaust, as the off-gas exists through this pathway. Heat was assumed to pass to the intumescent layer and the manifold cover through conduction, convection, and radiation. Heat was also assumed to conduct through the cover attached to the sides of the block. Additionally, heat loss to the atmosphere from the manifold cover was assumed to be through convection and radiation.

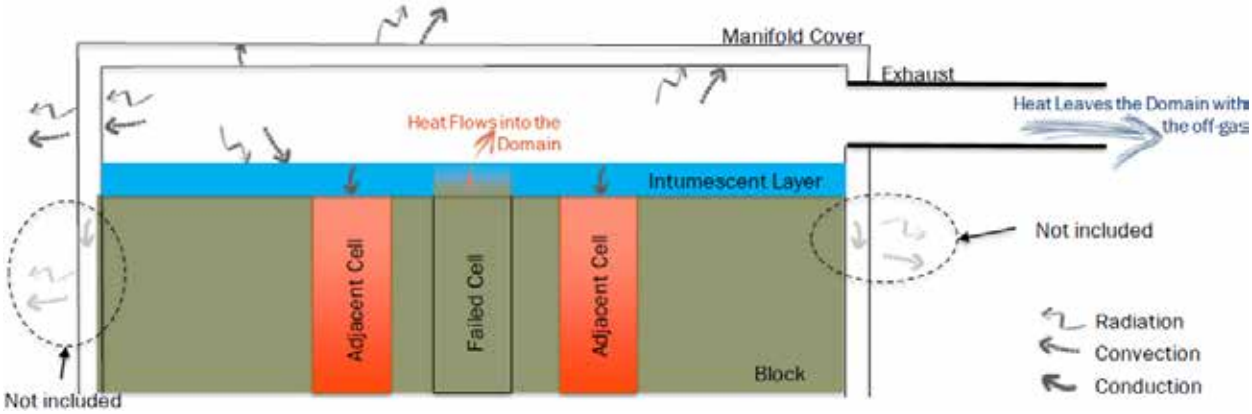

Figure 7. Illustration of heat transfer paths in the 1D model

A steady state analysis was performed to determine the viability of the design and determine whether choke points could exist which would retard flow, increasing heat transfer as well as allowing pressure to build in the setup. DNV GL's experience in other business areas has suggested that airtight systems with similar dedicated exhaust plenums may be insufficient beyond failure of a single cell. Given that off-gas must be managed, as opposed to vented into the aircraft space, the Pyrophobic material should aid in restriction of conductive heat transfer, and thus failure propagation. The primary findings from the exhaust sizing optimization were that:

- An exhaust duct diameter of 0.25”, regardless of length, is dangerously close to reaching Mach 1 (lower Mach number is better) through the tube and thus running the risk of a choked flow.
- The tube length had minimal to no influence in the Mach number.
- The diameter of the tube poses a logarithmic increase in Mach number as the diameter decreases.
- Mach number increases with increasing temperature. Though temperatures above 800 °C are common during combustion with thermal runaway, DNV GL has observed higher temperatures in confined spaces, suggesting yet a higher Mach number.
- Manifold pressure increased logarithmically with decreasing diameter. As temperature increases to combustion ranges, pressure in the manifold may reach 20 psi or higher for a 0.25” exhaust diameter, potentially approaching dangerously high static pressures within the system.
- Should the failure propagate to all cells, or even beyond the five-cell cluster, and include cells in other similarly facing groups, choked flow conditions would almost be inevitable.
- By doubling the exhaust duct diameter from 0.250” to 0.500”, Mach number at exit, even for total failure, decreased by over half, to under 0.4, while pressure in the manifold decreased by an order of magnitude. If the exhaust diameter is increased to 0.750” again, pressure decreased by an order of magnitude, while also reducing Mach number by half, to 0.18 with a seven cell failure.

As discussed above, exhaust duct diameter was identified as a critical parameter for safety consideration. A diameter of 0.250” puts the battery pack dangerously close to reaching Mach 1 through the tube and thus running the risk of a choked flow, and resulting in high exhaust manifold pressure. Increasing the exhaust duct diameter significantly alleviates the safety risk.

3.2 Cell block design

This section discusses battery cell block design work performed by TTWAS; it is a continuation of the 1D analysis described in the previous section. 1D modelling was used to perform steady state venting analysis, which provided exhaust duct constraints. This section presents the second part of the modeling exercise focused on transient venting analysis with heat transfer and exhaust restriction.

The output of this analysis provided the interfacial temperature at the inside faceplate of the Pyrophobic material where it contacts the battery vent. This analysis is a revision of the previous work with blockage of the exhaust duct and provides backpressure, flow, and interfacial

temperature data in cases where some percentage of the exhaust duct was blocked; either as a result of the intumescent material swelling, or debris from the batteries or the block being ejected into the manifold space. Though DNV GL theorized the intumescent material a more likely culprit in restricting gas flow, the FAA has reported the ejection of battery materials, including vent caps, rings, and “jelly roll” material that has blocked exhaust ducting in their tests.

The solid components of the battery pack include the battery, block, intumescent layer, and the manifold cover. Gas leaving the batteries was assumed to traverse the full length of the manifold or 10.6” and make only one pass without recirculation. The model also assumed that there was no heat transfer into adjacent batteries due to electrical connections. Forced convective heat transfer was assumed in the manifold during the off-gas release; after the release of the off-gas stopped, it switched to natural convective heat transfer. DNV GL also requested additional analysis from TTWAS to assess the implications on transient warming of adjacent batteries when the manifold may be blocked by expanding intumescent material, restricting movement of off-gas into the exhaust.

The analysis considered five and seven cells undergoing thermal runaway with various exhaust diameter restrictions. Analysis of the unrestricted transient flow showed that temperature increase at the interfacial boundary of the cells and the intumescent material did not exceed 10 °C (up to 70 °C from an initial interfacial boundary temperature of 60 °C). This is explained by a lack of back pressure in the manifold restricting flow and allowing for increased conductive and convective heat transfer, while minimizing the time for heat loss through the manifold. This minimal temperature increase indicated that the temperature impacts on adjacent cells is low in the unrestricted exhaust flow case.

The restricted exhaust flow analysis considered scenarios with 25%, 50%, and 75% blockage of the exhaust inlet. Despite the build-up in back pressure as a result of the blockage in the exhaust manifold, the results indicated that interfacial temperatures were still within safe limits. Thermal runaway of adjacent batteries is not expected based on this result. However, the results did indicate very high manifold back pressures due to the blockages, reaching 79.5 psig for a 7-cell failure with a 75% restriction (see Table 4). While it is unclear how the batteries will continue to produce off-gas under such high-pressure conditions, these conditions, if achieved, would most likely result in the mechanical destruction of the manifold and intumescent block. Though the manifold design for this project is undefined with regard to structural strength, a risk analysis should be conducted to determine the likely worst-case failure scenario and design of the manifold should consider required rupture strength necessary to withstand such a failure.

Table 4. Max manifold pressures for a number of failure modes

# Batteries	Restriction	Release duration (sec)	Max pressure (psi-gauge)
5	25%	10	0.5
5	50%	10	1.7
5	75%	10	17.9
7	25%	10	0.9
7	50%	10	3.0
7	75%	10	31.5
7	75%	5	79.5
7	75%	25	6.4

4 Prototype test and validation

4.1 Demonstrate off-gas control logic in BMS

DNV GL assessed how the early detection Li-ion Tamer sensor from Nexceris performed with the prototype battery module, where batteries were subject to failure conditions within Pyrophobic blocks made of intumescent material. DNV GL performed four tests using two types of Pyrophobic blocks to validate performance of the Nexceris sensor. The battery module was enclosed within a metal enclosure to contain off-gas from failed cells and direct it through an exhaust.

The four tests utilized off the shelf Samsung SDI-26J battery cells rated at 2.6 Ah with a nominal voltage of 3.63 V. The tests were performed in two types of Pyrophobic battery module blocks each designed to hold 36 cells. The blocks and their corresponding lids are shown in Figure 8 and Figure 9 below.

- The Type 1 Pyrophobic block, shown in Figure 8, was designed to allow off-gas to vent through the lid through four small holes within the spherical space directly above each cell.
- The Type 2 Pyrophobic block design, shown in Figure 9, included small holes on the lid adjacent to each cell, through which off-gas is redirected via a vent path. Unlike the Type 1 block, the openings in the lid are not situated directly over each cell. The expectation is

that a longer tortured path of the Type 2 block should have less fire ejecting through the lid, as the path will cool the electrolyte before being released into the atmosphere.

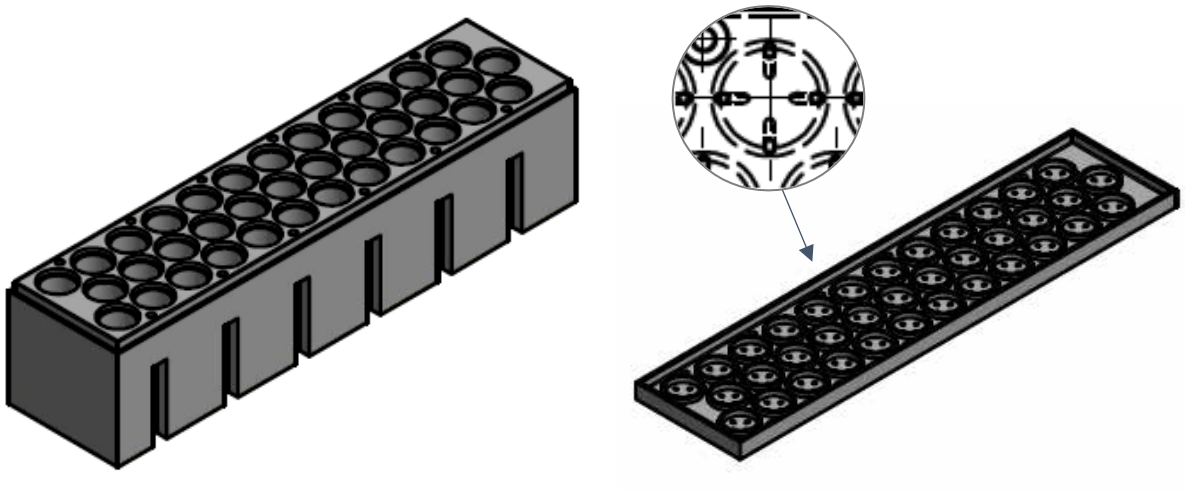

Figure 8. Pyrophobic cell block and lid - Type 1

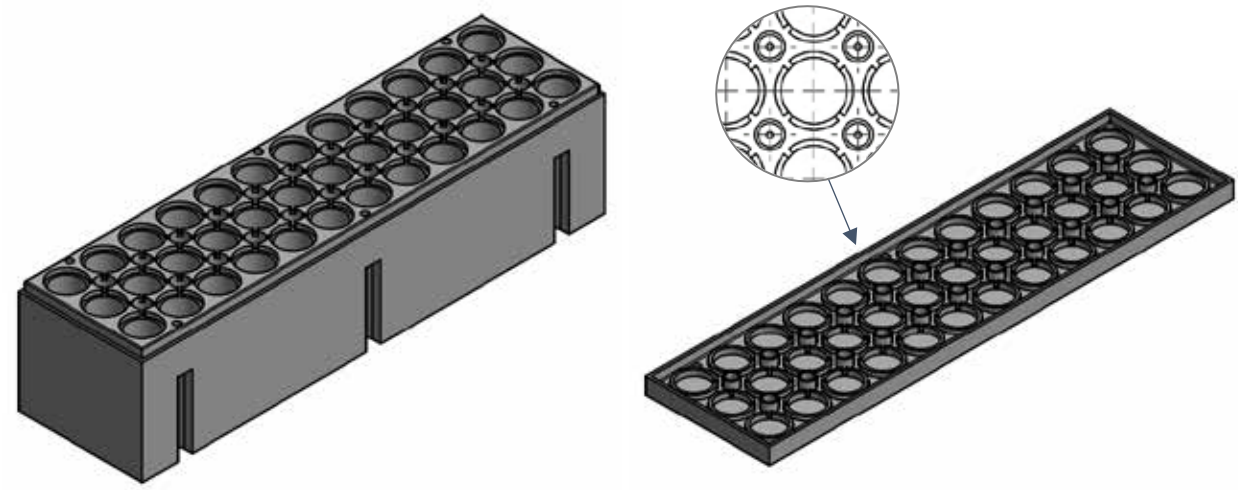

Figure 9. Pyrophobic cell block and lid - Type 2

Both Type 1 and Type 2 Pyrophobic blocks were placed in a metal enclosure constructed of 0.060” thick material and designed to be flush with the Pyrophobic cell block on all sides with one exception. The area above the lid of the cell block included a 1.5” headspace for gases to exhaust. The exhaust is designed with two openings that are ¾” and 1” in diameter, as shown in the left section of Figure 10 below.

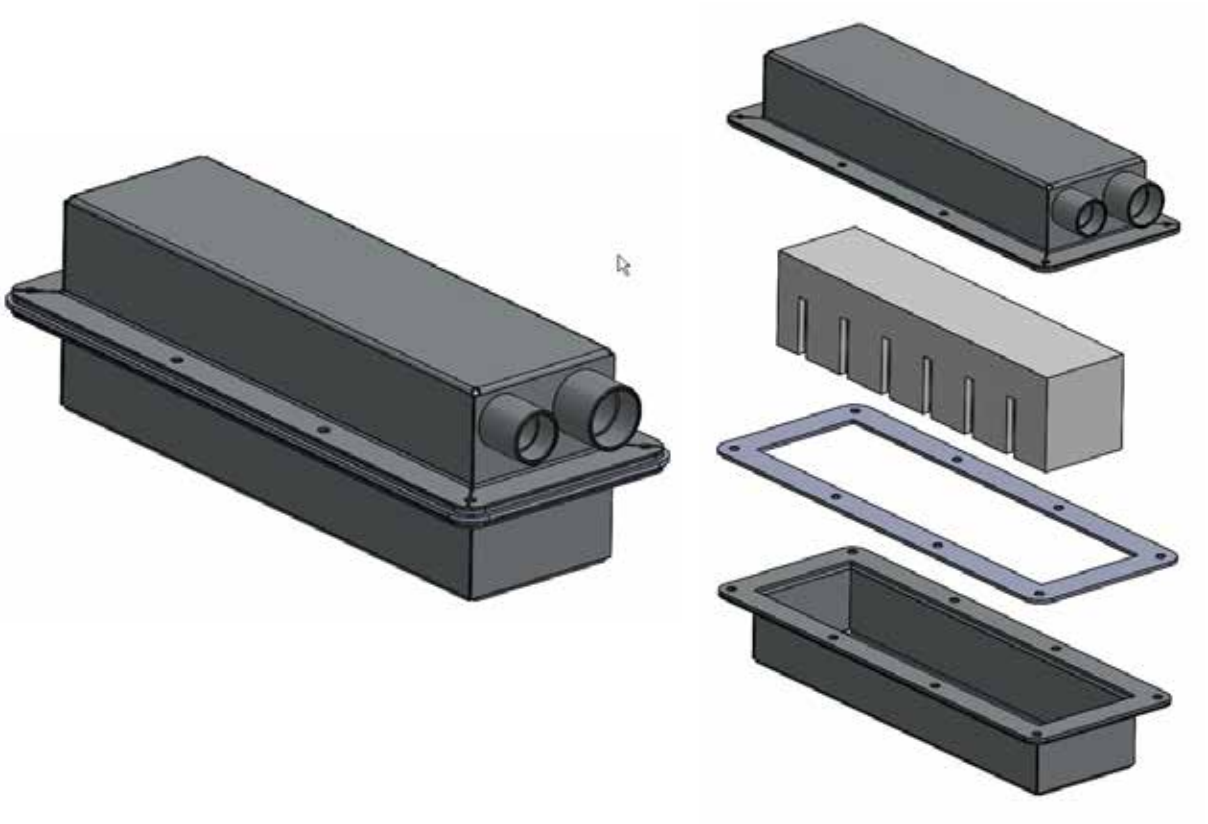

Figure 10. Exhaust manifold cover with exploded view

Lastly, the Nexceris Li-ion Tamer early detection sensor was placed downstream from the battery module enclosure in the exhaust pipe as shown in Figure 11. The Nexceris sensor was placed approximately 43.5” (3.6 ft.) as measured from the farthest end of the battery module enclosure or 30” (2.5 ft.) away from the beginning of the exhaust pipe of the battery module enclosure.

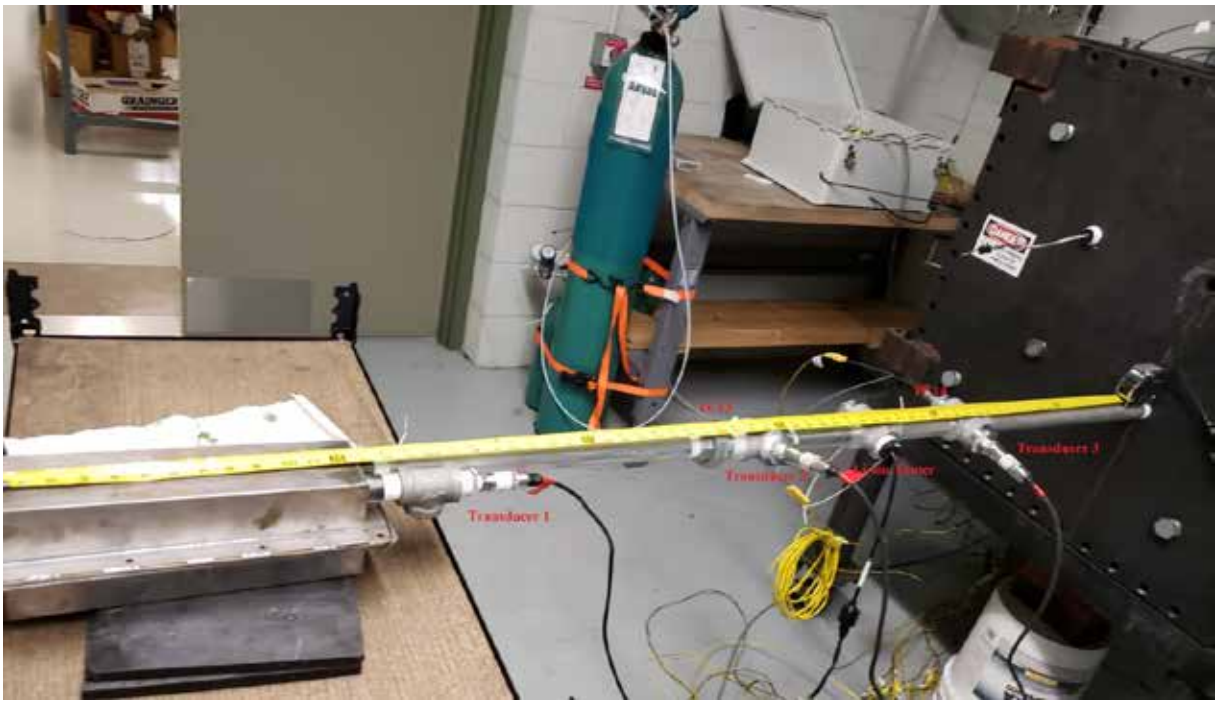

Figure 11. Nexceris Li-ion Tamer sensor placement

A summary of the four tests' set-ups is shown in Table 5 below, which describes the number of cells that were subject to failure through overheat, number of adjacent cells, exhaust manifold opening used, and the type of Pyrophobic block used.

Table 5. Test setup summary

Test	Pyrophobic block	Heated cells	Cells without heat applied (adjacent)	Exhaust manifold opening	Exhaust pipe	
					Length	Pipe #
1	Type 1	2	8	1"	~70"	1
2	Type 2	2	6	1"	~70"	1
3	Type 1	2	8	3/4"	~70"	2
4	Type 2	2	6	1"	~70"	1

Test 1 and Test 3 used the Type 1 Pyrophobic block with eight adjacent cells around two heated cells, as shown in Figure 12 for Test 1. Each test set-up included up to 14 thermocouples (TC1 – TC14) for temperature measurements. TC1 recorded the temperature of one of two cells subject to overheat whereas TC2 – TC7 were placed on six, non-heated, adjacent cells. For all four tests,

TC8 and TC9 measured temperature at the top of the Pyrophobic lid, also described in the figures below as Pyrophobic channel, while TC10, TC11, and TC12 measured the temperature of the metal enclosure above the Pyrophobic channel. The temperature inside the exhaust pipe was measured by TC13 and TC14.

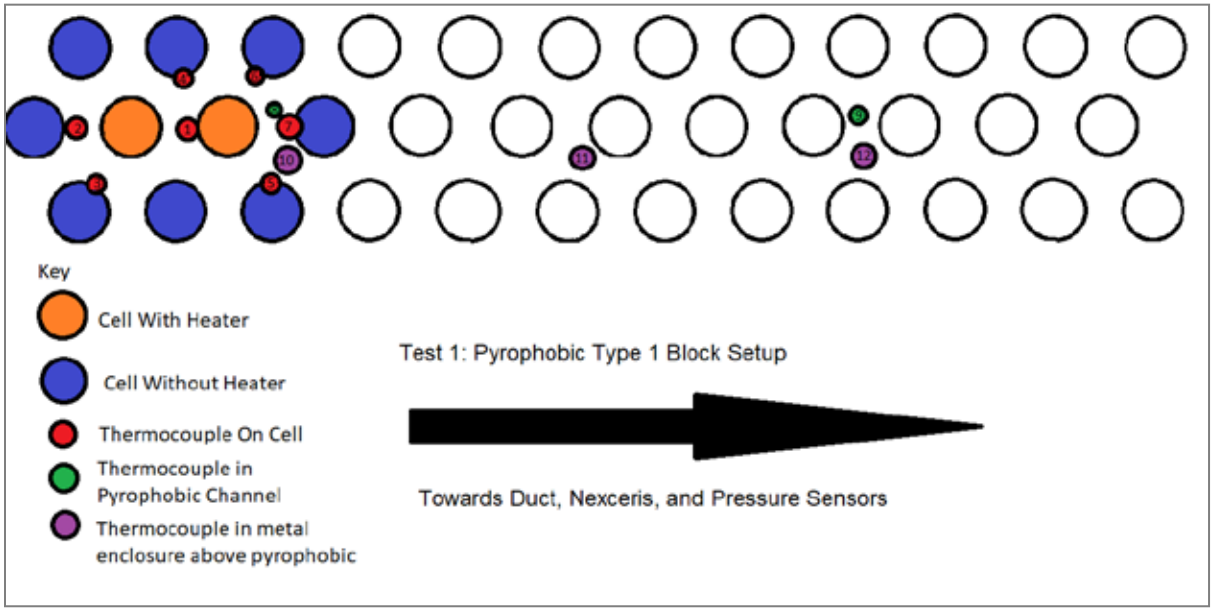

Figure 12. Test 1 setup

Test 2 and Test 4 used the Type 2 Pyrophobic block with six adjacent cells around two heated cells, as shown in Figure 13 for Test 2. The temperatures of both heated cells were measured by TC1 and TC2 while the temperatures of five of the adjacent cells were measured by TC3 – TC7. The placement of TC8 – TC14 were the same as described for Test 1 and Test 3 above.

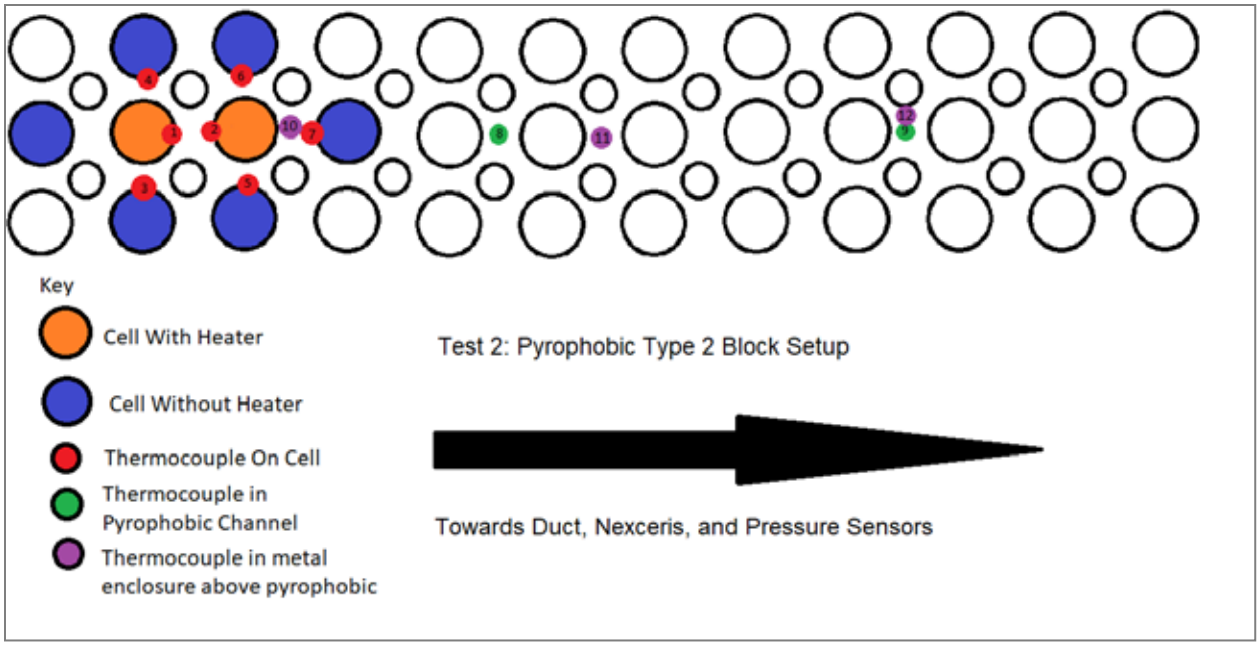

Figure 13. Test 2 setup

Figure 14 shows the temperature of one of the heated cells as measured by TC1 for Test 1. The plotted data indicates that the heated cell started to vent off-gas at 7.19 minutes, which is highlighted by a decrease in temperature, and went into thermal runaway at 7.23 minutes. The temperature of the cell increased from 146 °C to 1,203 °C in 1.98 seconds. A pressure spike was observed at 7.21 minutes, 1.02 seconds prior to thermal runaway. However, the Nexceris Li-ion Tamer sensor was triggered approximately 3 seconds after the cell went into thermal runaway, concurrently with the cell reaching peak temperature.

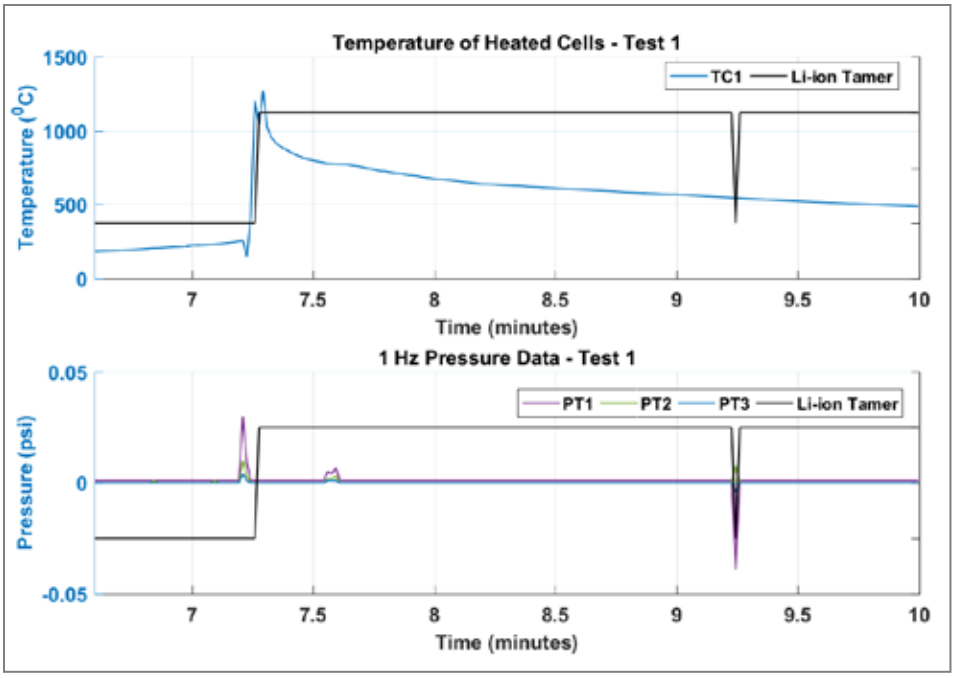

Figure 14. Temperature of the heated cell and pressure characteristics for Test 1

Figure 15 shows the temperatures of the heated cells as measured by TC1 and TC2 for Test 4. In Test 4, the heated cell measured by TC1 went into thermal runaway at 7.07 minutes where the temperature of the cell increased from 204.6 °C to 2,293 °C in 1.02 seconds. The high temperature observed here indicates that the cell vented violently or combusted without exothermic consumption. Based on the data, the cell connected to TC1 likely started to off-gas around 6.48 minutes or approximately 35 seconds prior to the thermal runaway event. The second heated cell started to off-gas even earlier at 6.05 minutes and went into thermal runaway at 7.05 minutes, where temperature of the cell increased from 119.9 °C to 853.7 °C over a period of 9.96 seconds. Test 4 results also indicated that the Nexceris Li-ion Tamer sensor was triggered immediately after thermal runaway started, and concurrently, or slightly before, the cell reaching peak temperature.

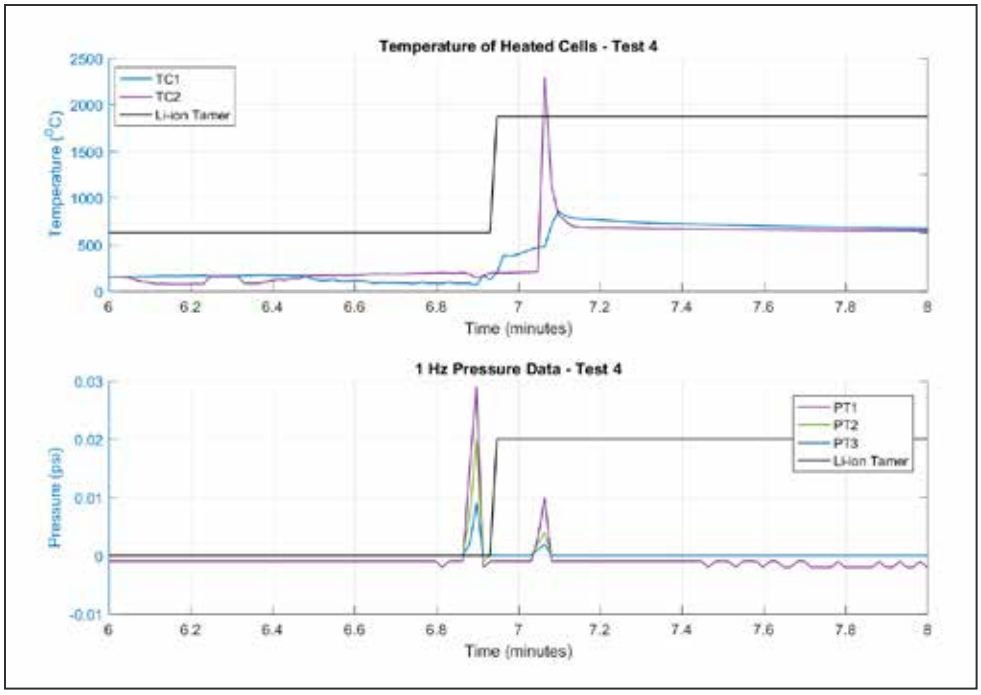

Figure 15. Temperature of the heated cells and pressure characteristics for Test 4

Off-gas detection test results are summarized in Table 6 below. Test 1 and Test 3 results include the Type 1 block design, while Test 2 and Test 4 results include the Type 2 block design. In all Tests, the Li-ion Tamer sensor was triggered immediately after thermal runaway started, and concurrently with, or slightly before, the heated cell reaching peak temperature.

Table 6. Off-gas detection test results summary

Test	**Temperature characteristics**				**Pressure**	**Off-gas sensor**
	Elapsed time at start of thermal runaway (min)	Temp. at start of thermal runaway (°C)	Elapsed time at peak temp. (min)	Peak temp. (°C)	Elapsed time at peak pressure (min)	Elapsed time at Li-ion Tamer trigger (min)
1	TC1: 7.227	146.3	7.260	1,203.0	7.210	7.277
3	TC1: 7.386	221.3	7.486	421.7	7.403	7.436

Test	Temperature characteristics				Pressure	Off-gas sensor
	Elapsed time at start of thermal runaway (min)	Temp. at start of thermal runaway (°C)	Elapsed time at peak temp. (min)	Peak temp. (°C)	Elapsed time at peak pressure (min)	Elapsed time at Li-ion Tamer trigger (min)
2	TC1: 23.68	246.5	23.85	673.7	23.70	21.93
2	TC2: 23.53	241.0	23.55	554.4	23.55	
4	TC1: 6.932	119.9	7.098	853.7	6.898	7.065
4	TC2: 7.048	204.6	7.065	2,293	7.065	

Table 7 provides a summary of the time when the Li-ion Tamer sensor was first triggered and the point at which a heated cell started to go into thermal runaway. Early detection using the off-gas sensor was only successful in Tests 2 and 4. Both of these tests were performed in the Type 2 Pyrophobic block, which featured a longer tortured path for the off-gas before it vented out of the block and into the exhaust manifold. Test 2 was considered an outlier, and likely had an erroneous reading from the early detection sensor given that the heaters were switched on and off a few times during the test. The level of detection by the Li-ion Tamer sensor in these tests is different compared to the initial testing performed on individual cells, which were not subject to the same testing conditions.

Table 7. Li-ion Tamer sensor detection

Test	Pyrophobic block	Li-ion Tamer detection	Start of thermal runaway (first cell)	Difference
1	Type 1	7.28 mins	TC1: 7.23 mins	+3 seconds
2	Type 2	15.4 mins	TC2: 23.53 mins	-487 seconds
3	Type 1	7.39 mins	TC1: 7.44 mins	+3 seconds
4	Type 2	6.95 mins	TC2: 7.05 mins	-6 seconds

The Nexceris sensor was not able to provide early detection of off-gas release as expected through the battery module prototype in half of the cases. The Type 2 Pyrophobic block did allow early detection of off-gas; however, the time between detection and thermal runaway varied significantly between both tests that were performed using this block type. The Type 1 Pyrophobic block on the other hand provided detection three seconds after the first cell in each test underwent thermal runaway. Without any added airflow from exhaust fans, the Type 1 Pyrophobic block may have caused off-gases to linger within itself for a longer period, which may have prevented gases from being detected by the Li-ion Tamer sensor that was placed downstream.

DNV GL noticed that erroneous temperature data were being recorded when the heater was turned on. In order to fix this issue, the heater was turned off, which allowed for more consistent temperature data measurement. However, the heater had to be turned on again for short periods in order to bring the temperature of the cells up to conditions that would facilitate thermal runaway.

4.2 Verification of cascading prevention

DNV GL assessed how well the Pyrophobic block with its intumescent material was able to prevent cascading of thermal runaway from heated cells to adjacent cells. DNV GL performed four tests using the Type 1 and Type 2 Pyrophobic blocks and thermocouple placements described previously; Tests 1 and 3 used the Type 1 block, while Tests 2 and 4 used the Type 2 block. During each test, the battery module was placed within a metal enclosure to contain off-gas from failed cells and direct it through an exhaust.

In each of the four tests, two cells were heated until the cells entered thermal runaway and the temperature of non-heated adjacent cells was monitored. This approach facilitated the evaluation of cascading prevention provided by the intumescent block design. Figure 16 shows the temperature measurements for Test 1; TC2 – TC7 represent the temperature of adjacent cells. During the test, the heated cell reached a temperature of 1,271 °C; however, the adjacent cells only experienced a brief spike in temperature, with a maximum 262 °C. The temperature of adjacent cells stayed in a reasonable range of 30 °C – 62 °C before and after the heated cells reached thermal runaway. The spike in temperature of adjacent cells only lasted for around 2 seconds; the short duration of temperature peaks in the adjacent cells is likely due to material properties of the Pyrophobic block. These results indicate that the Pyrophobic block prevented enough heat from being transferred from the faulted cell to adjacent cells, thus preventing cascading of thermal runaway.

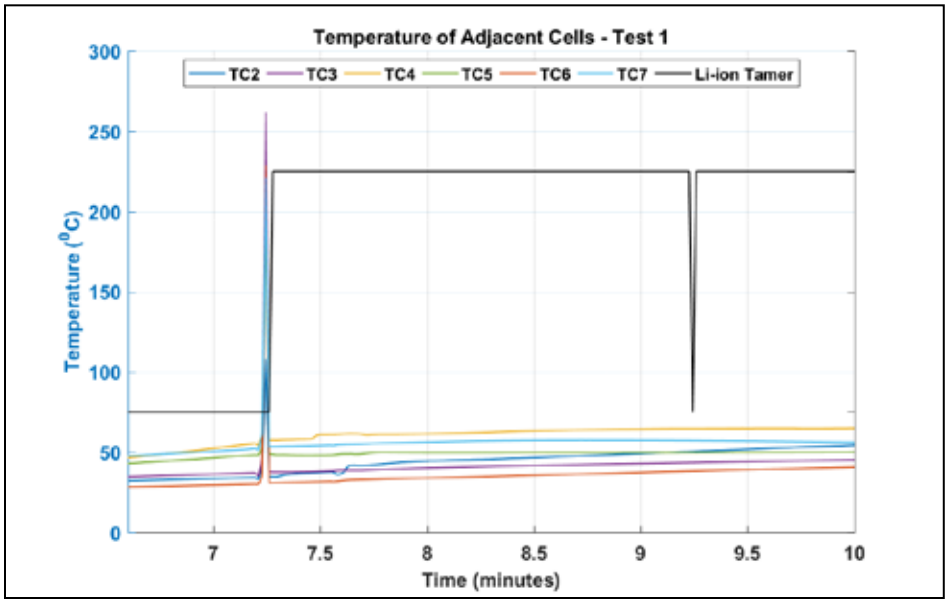

Figure 16. Cascading prevention: temperature of adjacent cells in Test 1

Figure 17 shows the temperature of five adjacent cells in Test 2; peak temperatures for heated cells measured by TC1 and TC2 were 698.2 °C and 731.9 °C, respectively. The highest temperature that an adjacent non-heated cell reached was 121 °C. This is a good indication that the Pyrophobic block prevented heat transfer from the heated cells to adjacent cells, thereby preventing additional thermal runaway events. The temperature of the adjacent cells at the beginning of Test 2 were in the range of 46.3 °C – 80.1 °C. These temperatures are relatively higher than those observed in Test 1, which could be due to a difference in the type of Pyrophobic block used. After the heated cells had gone into thermal runaway, the temperature of the adjacent cells increased further before dropping. Based on the results from Test 1 and Test 2, the Type 2 Pyrophobic block did not perform as well as the Type 1 Pyrophobic block in terms of containing heat transfer. However, the Type 2 Pyrophobic block still provided adequate cascading prevention as no thermal runaway occurred in the adjacent cells. During thermal runaway, TC5 and TC6 displayed the highest temperatures, as these cells were located closest to the heated cells.

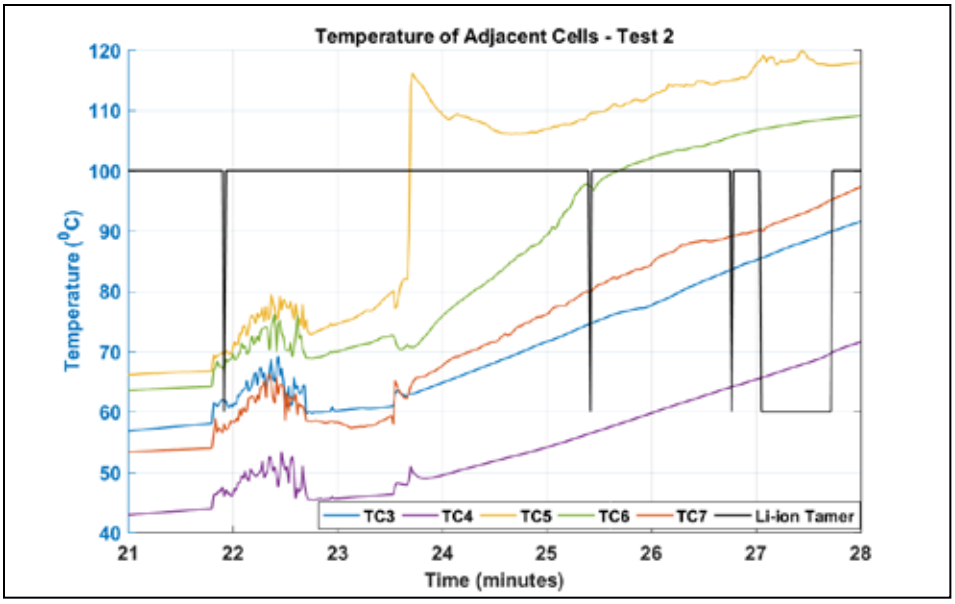

Figure 17. Cascading prevention: temperature of adjacent cells in Test 2

The testing also included cell voltage measurements and physical observation after each test. The results were in line with those of the temperature measurements described previously. The intumescent material block offered cascading prevention; however, the Type 1 block offered better protection than the Type 2 block.

DNV GL measured voltage of one of the heated cells and all eight adjacent cells for Test 3, as shown in Table 8. The nominal voltage of tested cells are 3.63 V. The voltage measurement shows that the heated cell is damaged, and all adjacent cells remain undamaged.

Table 8. Cascading prevention: voltages of adjacent cells Test 3

Cell Type	Cell	Voltage (V)
Heated Cell	1	0.016
Adjacent Cell	1	4.131
Adjacent Cell	2	4.127
Adjacent Cell	3	4.124
Adjacent Cell	4	4.125
Adjacent Cell	5	4.126
Adjacent Cell	6	4.129
Adjacent Cell	7	4.127
Adjacent Cell	8	4.127

Figure 18 shows the state of heated cell and adjacent cells from Test 3. The heated cell ejected through the Pyrophobic lid; however, similar damage was not observed in any of the adjacent cells. Wood fillers in this block show little deposits of cell material that entered through the lid and settled on top of each cell. None of the adjacent cells were damaged and the combusted material coming out of the heated cell was primarily found closest to itself.

Figure 18. Physical overview of block after Test 3

The Pyrophobic blocks were able to prevent cascading of thermal runaway from overheated cells to adjacent cells. This was made evident through temperature measurements of adjacent cells, which were considerably lower than the heated cells. The design of the Type 2 block likely caused excessive build-up of hot gases from overheated cells and damaged neighboring cells. Overall, the Type 1 Pyrophobic block displayed better cascading prevention and failure containment capabilities than the Type 2 Pyrophobic block.

DNV GL noticed that erroneous temperature data were being recorded when the heater was turned on. In order to fix this issue, the heater was turned off which allowed for more consistent temperature data measurement. However, the heater had to be turned on again for short periods

in order to bring the temperature of the cells up to conditions that would facilitate thermal runaway.

Based on data from these four tests, the Pyrophobic blocks managed to prevent cascading of thermal runaway to adjacent cells; however, cell failure was not limited to only the heated cells. Adjacent cells in some cases were physically damaged, though not nearly to the same extent as heated cells. To further verify the effect from heat exposure on adjacent cells, DNV GL would recommend measuring mass and voltages for each cell before and after the tests.

4.3 Verification of heat dissipation

As with the off-gas detection and cascading prevention discussed previously, DNV GL performed four tests—Test 1 and 3 using a Type 1 intumescent block and Test 2 and 4 using a Type 2 Pyrophobic block—to verify heat dissipation in the battery module made with the Pyrophobic material and its ability to mitigate the impact of thermal runaway of Li-ion cells on adjacent cells. During each test, the battery module was placed within a metal enclosure to contain off-gas from failed cells and direct it through an exhaust. The exhaust utilized a round pipe approximately 70’’ long and 1’’ in diameter.

Temperature results for Test 1 are shown in Figure 19, Figure 20, and Figure 21 below. The measurements shown are:

- TC1 – temperature of a heated cell;
- TC2 to TC7 – temperature of adjacent non-heated cells;
- TC8 – thermocouple on top of the Pyrophobic block lid, within an inch of the heated cells;
- TC9 – thermocouple on top of the Pyrophobic block lid, 6 inches from heated cells;
- TC10 to TC12 – temperatures across the ceiling of the metal testing enclosure; and
- TC13 and TC14 – thermocouples in the exhaust pipe approximately 35 and 50 inches away from the heated cells, respectively.

The results show the temperature of the heated cell reaching thermal runaway at about 7.4 minutes and then gradually decreasing in heat over the next 20 minutes. At the same time, a few of the adjacent cells reached temperatures just above 250 °C for less than 2 seconds before coming down quickly to under 80 °C for the remainder of the test. The temperatures recorded on the top of the Pyrophobic block lid also showed momentary spikes coinciding with the heated cell reaching thermal runaway; TC8 was likely damaged from the thermal runaway event, which

resulted in faulty readings. The temperatures across the ceiling of the metal enclosure rose to about 500 °C when the heated cells were in thermal runaway and gradually dropped over time. TC10 was positioned closest to the heated cells, which is why its temperatures were higher and took longer to decrease compared to TC11 and TC12. The thermocouples in the exhaust pipe also rapidly increased due to the thermal runaway event; however, exhaust temperatures did not rise above 100 °C and cooled down to ambient levels within a relatively short period of time. Similar results were observed for Tests 2, 3, and 4.

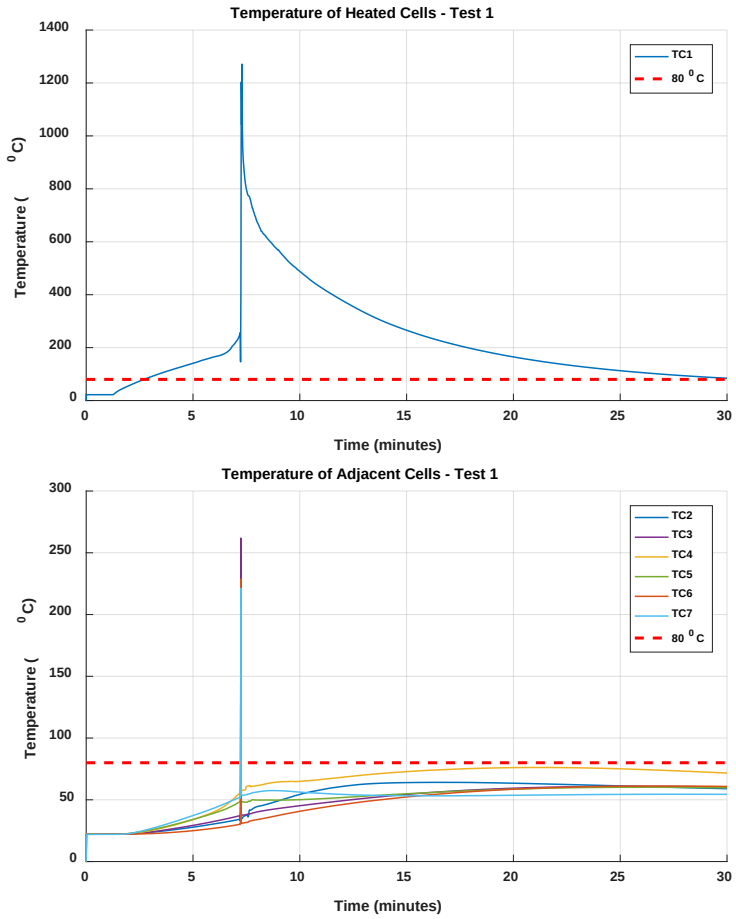

Figure 19. Heat dissipation: heated and adjacent cells – Test 1

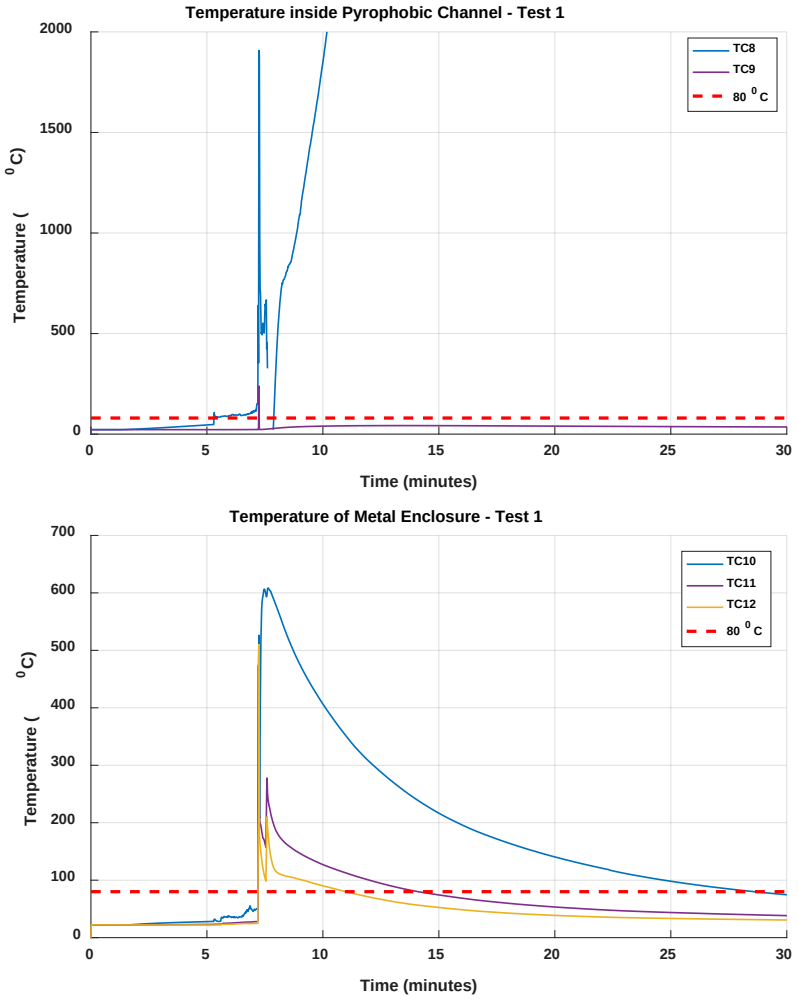

Figure 20. Heat dissipation: temperatures on Pyrophobic lid and ceiling of metal enclosure – Test 1

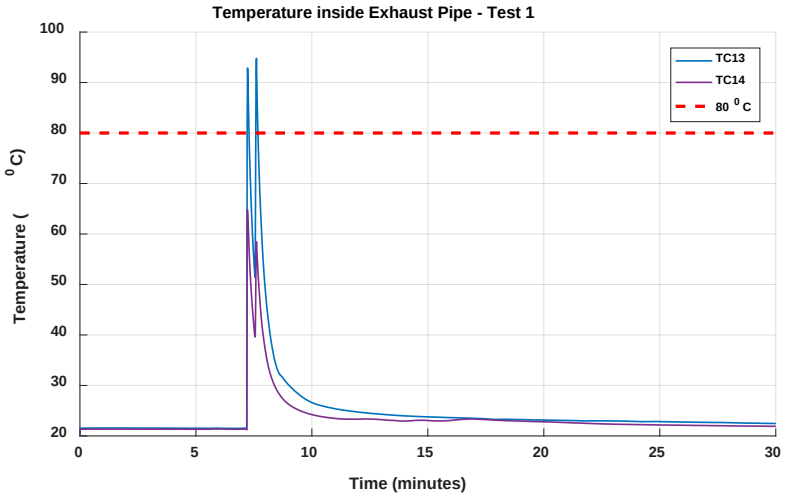

Figure 21. Heat dissipation: exhaust pipe temperatures – Test 1

The rapid drop in temperature of the adjacent cells after thermal runaway occurred in the heated cells and the increase in Pyrophobic material surface temperature indicate that the Pyrophobic block is able to dissipate heat and reduce the risk of adjacent cells reaching thermal runaway. Based on the findings from these tests, the proof of concept of the overall manifold design and design for containment was successful. The intumescent Pyrophobic material facilitated heat dissipation through the system and maintained lower temperatures during thermal runaway conditions compared to surfaces like the exhaust manifold metal enclosure. While most of the heated cells underwent thermal runaway conditions, their neighboring cells were able to maintain lower temperatures due to conductive properties of the Pyrophobic material, which helped prevent cascading of thermal runaway. As expected, temperatures of thermocouples downstream from the heated cells on the metal enclosure dissipated quickly compared to thermocouples placed close to the heated cells. Lastly, the diameter of the exhaust pipe had an impact on temperatures in that the exhaust pipe, with a smaller opening resulting in much higher gas temperatures as they were exiting the battery enclosure.

4.4 CAB acceptance checklist

DNV GL prepared acceptance criteria and templates to outline the appropriate reporting methodology by which compliance with design standards could be confirmed with this advanced battery module system as it scales for production/use, or to verify future evolution of design, as alternative suppliers or equipment become commercially available.

Although the design may evolve by necessity, the end goal will remain the same: for the safe operation and, in the case a failure event occurs, failure management of energy storage systems in an aircraft. As such, the following areas have been selected for verification regardless of supplier, subcomponents, or configuration:

- Resistance to or prevention of thermal runaway/hazardous battery failure
- Resistance to or prevention of cascading thermal runaway/battery failure to adjacent batteries
- Containment of failure event within specified area
- Management of failure event impact external to specified area
  - Fire/heat
  - Pressure
  - Toxicity
- Monitoring and operational continuity in a failure event

Appendix A provides an example template for acceptance criteria.

4.5 Delivery of design package for CAB

DNV GL prepared design package requirements to outline the central design objectives leveraged for this prototype, to allow future adoption of this design with identical or alternative suppliers and equipment. As such, this design package is intended to support the adoption and evolution of the production of flight-safe energy storage systems, based on the learnings of this research effort.

The intention of the design is to:

1. Prevent a failure event from occurring
2. Limit the impact of a failure event such that the aircraft is not affected
3. If the battery is supporting a flight critical system, continue operation until it is possible to safely land, or, if it is not flight critical, gracefully shut down the system.

Further details are provided in Appendix A.

5 Evolving standards and innovative applications

As part of this study, DNV GL assessed how the battery module prototype could be contextualized with the evolving standards environment and for innovative applications such as urban air mobility. DNV GL reviewed standards currently applicable to battery systems on aircrafts and provided considerations for anticipated future needs as their applications evolve.

The Code of Federal Regulations (CFR) provides guidance for battery systems through its airworthiness standards for transport category airplanes such as unmanned aircraft systems (UAS), which is also known as part 25[3]. The airworthiness standard currently specifies the use of battery systems in a few areas: engine ignition systems (§25.1165), electrical equipment and installations (§25.1353), and emergency lighting (§25.812).

Some of the key items in the standard pertaining to batteries are provided within this review. For engine ignition systems, section (g) specifies that there must be a means to warn crewmembers if the malfunctioning of any part of the electrical system is causing the continuous discharge of any battery necessary for engine ignition. For electrical equipment and installations, section (b) specifies that storage batteries must be designed and installed such that: safe cell temperatures and pressures are maintained without an uncontrolled increase in cell temperature after the battery is recharged; battery performance must be shown to comply with safe operation through testing and experience from prior installations; no explosive or toxic gases emitted by any battery may accumulate in hazardous quantities within the airplane; and no corrosive fluids or gases that may escape from the battery may damage surrounding airplane structures or essential equipment. Section (b) also provides guidance specifically for legacy NiCd battery technology, which states that their installation must have provisions to prevent any hazardous effect on structure or essential systems, a system to control their charging rate, and a temperature and failure sensing system with a means of disconnecting the battery from its charging source.

While the existing guidelines in 14 CFR part 25 seek to enable safe operation of battery systems within aircrafts, new aspects should also be considered as the use of UAS grows and advancements are made in the emerging field of advanced aerial mobility (AAM). Key applications within AAM include urban air mobility (UAM), air passenger, and cargo transportation within urban or peri-urban areas with vehicles ranging from small drones to passenger aircrafts. UAM can include urban air taxis, enabled by electric vertical take-off and landing (eVTOL) capability, and cargo delivery aircraft, which are currently being researched and developed by many commercial entities. The relation of advanced aerial mobility and UAM application is captured in Figure 22 below[4].

[3] Electronic Code of Federal Regulations, Part 25 – Airworthiness Standards: Transport Category Airplanes. https://www.ecfr.gov/cgi-bin/text-idx?node=14:1.0.1.3.11

[4] National Academies of Scienes, Engineering, and Medicine 2020. *Advancing Aerial Mobility: A National Blueprint*. Washington, DC: The National Academies Press. https://doi.org/10.17226/25646

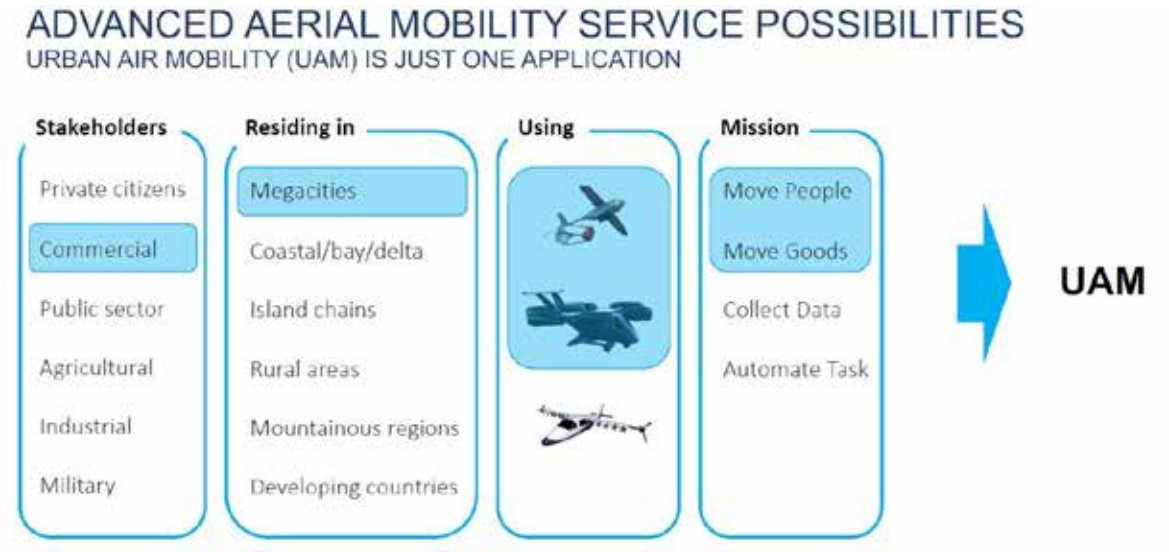

Figure 22. Advanced aerial mobility and urban air mobility overview

The battery module design examined through this study was as an example to meet best current industry for UAS safety practices guidelines. This is made possible through features such as the intumescent material to prevent cascading of thermal runaway, as well as an early detection sensor to provide warning of battery cell failure. Specifically, the prototype battery module design adheres to part 23, 25, 27 and 29 guidelines by maintaining safe cell temperatures, limiting accumulation of explosive or toxic gases from batteries, and utilizing a temperature and failing sensing system with a means to disconnect the battery from its charging source.

As the need for UAS expands in commercial settings, it is important that their reliability and safety is guided through standards and regulations. Currently, 14 CFR part 107 provides guidance on the operation of small UAS weighing less than 55 pounds for applications other than recreation or hobby purposes. However, current civil airworthiness or operational standards do not address large UAS for urban air mobility applications such as urban air taxis and cargo delivery aircraft, highlighting the need to establish standards. While critical features of UAM, such as detect and avoid (DAA), Command and Control (C2), and UAS Traffic Management (UTM), are being researched by the FAA and its partners, consideration shall be given to topics related to battery storage systems in anticipation of future UAM needs.

Topics for consideration in future standards for UAM may include establishing operational redundancies, environmental considerations such as emissions requirements for aircrafts with battery technologies, and battery end of life management. Some of the concept models designed for urban air taxis dedicate a considerable amount of the aircraft’s weight for battery storage to

be used for propulsion. Future standards should consider lessons learned from testing and field performance of Li-ion batteries to establish redundancy in energy capacity in case a failure is detected in a battery cell, which may cause a module to fail. Currently, engine exhaust emissions are subject to 14 CFR part 34, which specifies fuel venting and exhaust emissions for turbine engine powered airplanes. With hybrid and all electric aircraft under development, future emission requirements should consider aircraft using battery storage for propulsion.

Lastly, widespread use of battery technologies in UAM will further add to the growing amount of batteries that have met their useful life and are subject to disposal. Future standards and requirements should consider how batteries should be managed once their useful life has been met. This may be achieved by properly recycling or disposing of batteries to limit their impact on landfills. Current battery disposal regulations consider batteries to be “universal waste” by the Environmental Protection Agency (EPA) in small quantities, and “hazardous waste” by the EPA in large quantities. They are required to be shipped via Department of Transportation (DOT) approved means (which includes compliance with UN/DOT 38.3 at beginning of life, in most cases). They are required to be handled specially (i.e., they cannot be dropped into a local garbage dump). However, there are not federal regulations on how they are to be handled beyond this. In fact, the Rechargeable Battery Management Act that was passed in 1992 to regulate the production and disposal does not include Li-ion technology; however, later regulations around universal waste (40 CFR Part 273) call it out. Some states do have regulations and requirements for batteries, but they are primarily focused on commercial products. As batteries increase in prevalence in UAM application, regulations specific to this use case will have to be developed.

In order to comply with some of the future standards described above, the battery module design examined through this study would need to be researched further. Multiple battery modules would need to be tested together in order to verify operational redundancies in the event that a module has failed, as well as to tie in the functionality of the BMS and controls. Future research of the battery module should include emissions monitoring as well as methods to repurpose or properly dispose of battery packs once they have met the end of their useful life on aircraft. Furthermore, the topics mentioned above may become part of performance-based standards to ensure safe, efficient, and reliable use for UAS for urban air mobility in the near future.

6 Conclusion

Over the course of this program, DNV GL tested a novel battery module design with the goal of mitigating cascading thermal runaway and providing early warning of failure. The program consisted of four major tasks including a background literature review, basic design testing,

modeling, and prototype testing. First, DNV GL performed a literature review to examine battery safety events in the industry, performance characteristics, hazards and codes that are relevant to Li-ion battery technology. During this task, DNV GL proposed a design strategy that entailed quantifying the thermodynamic and fluid dynamic behavior of battery off-gas. The computational fluid dynamics modelling was expected to guide the shape of exhaust plenums and manifolds required in the resulting battery module design. A design criteria or checklist was developed for a new battery solution design to fit within existing systems, as well as a punchlist of battery design criteria with actions for the commercial advisory board for adaptation.

Second, DNV GL performed basic design testing using off-the-shelf 18650 Li-ion cells in its battery testing facility. The tests were performed in two phases where initial testing included characterization of cells without the use of passive intumescent material and secondary testing incorporated the passive intumescent material, as well as off-gas early detection sensors. DNV GL examined cell behavior when caused to fail through overheat conditions and varied initial cell SOC between tests. Overall characteristics showed similar temperature behavior in all tests with observable correlations with higher initial SOC resulting in higher cell temperatures and higher mass loss. Additionally, measured gas concentrations were higher for tests performed in the tubular manifold test setup compared to the larger battery abuse chamber, which is likely due to a difference in volume.

These initial cell tests demonstrated higher energy density and shorter duration burns than previously studied by DNV GL. An inverse relationship was observed between cell physical size and peak temperature as smaller cells displayed higher peak temperatures per Ah. The 18650 cells were intense in their failure mode due to their constrained construction and high energy density: with short duration fires and high peak temperature per kg. With respect to early warning of cell failure, test results showed that the Nexceris Li-ion Tamer sensor was triggered several tens of seconds prior to thermal runaway in minimal to zero ventilation scenarios. The sensor, however, triggered concurrently with thermal runaway in two tests that included the intumescent material. In cases where a battery is flight critical, the incipient fault detection provided by the off-gas monitor could be communicated to the crew and allow them to decide how to proceed with the flight operations. Per the key findings of the preliminary testing, DNV GL changed the scope of modeling from finite element analysis of conductive heat transfer through the Pyrophobic intumescent material to computational fluid dynamics analysis of the gas release and escape.

During the third phase of the program, data from initial testing was used to produce models to modify cell block design and create refinements. The modeling work utilized a two-part

approach where initial modeling was performed through a 1D method, with more detailed CFD modeling being employed during final analysis. The CFD modeling was focused on flow and thermal modeling for battery thermal management and venting of gases released from cells under thermal failure conditions. A steady state analysis was performed to determine the viability of the design and whether choke points could exist that would retard flow, increasing heat transfer and building pressure in the setup. Exhaust duct diameter was identified as a critical parameter for safety consideration as a diameter of 0.250” put the battery pack dangerously close to reaching Mach 1 through the tube, thus running the risk of a choked flow, and resulting in high exhaust manifold pressure. The modeling exercise illustrated that increasing the exhaust duct diameter significantly alleviates the safety risk. The second part of the modeling exercise focused on transient venting analysis with heat transfer and exhaust restriction. Despite the build-up in back pressure because of the blockage in the exhaust manifold, the results indicated that interfacial temperatures were still within safe limits.

The last part of the program involved testing of the prototype battery module to evaluate off-gas control logic, verification of cascading prevention, and verification of heat dissipation. Four tests were performed using two variations of the intumescent material block. Tests indicated that the Li-ion Tamer sensor was not able to provide early detection of gas release as expected through the battery module prototype in half of the cases. Without any added airflow from exhaust fans, the Pyrophobic block may have caused off-gases to linger within itself for a longer period, which may have prevented the detection of gases by the Li-ion Tamer sensor that was placed downstream. Based on data from these four tests, the Pyrophobic blocks managed to prevent cascading of thermal runaway to adjacent cells; however, cell failure was not limited to only the heated cells. Adjacent cells in some cases were physically damaged, though not nearly to the same extent as heated cells. DNV GL suggests making improvements to the Pyrophobic blocks by increasing the thickness of the lid to prevent cells from ejecting through the module and to improve failure containment. Based on the findings from these tests, the proof of concept of the overall manifold design and design for containment was successful. The intumescent Pyrophobic material facilitated heat dissipation through the system and maintained lower temperatures during thermal runaway conditions compared to surfaces like the exhaust manifold metal enclosure. As expected, temperatures of thermocouples downstream from the heated cells on the metal enclosure dissipated quickly compared to thermocouples that were placed close to the heated cells.

A Appendix A: additional information

TASK 1.3 “DROP IN” BATTERY SOLUTION DESIGN CRITERIA

Drop in battery design criteria should include definitions for the criteria shown in Table 9. The table shows considerations for each criterion.

Table 9. Design criteria for battery system design

Design criteria		**Considerations**
Exterior dimensions of battery module		These specifications will be dependent on the aircraft in which the system will be implemented.
Containment		Self-containment in low-pressure environments.
Battery System weight		The weight will be dependent on the system criteria.
Battery Module Voltage		This will depend on the integration criteria from the aircraft systems, and how many battery modules will be required, and their series-parallel configuration.
Battery System Voltage		Same as above
Battery Module Current		Same as above
Battery System Current		Same as above
Maximum life considerations		The series-parallel configuration will have an effect on the capacity losses in the cells, as it governs the current and state of charge range the cell experiences.
Series-parallel configurations of cells (for optimum life and safety limits)		Related to above
Lowest cost considerations		The number of cells will determine the cost, which is dependent on the system geometry and series-parallel configuration.
Cooling		Air or conductive cooling will be determined by access to closed loop heat exchanger, and the size and mass of that system.
Required BMS criteria for system	Cell specific voltage limits	Depends on performance and safety requirements of cell.
	Cell specific current limits	Same as above
	Cell specific temperature limits	Same as above
	Error communication	May depend on on-board system communications criteria. Typical BMS language is CAN.
	BMS override of system commands	Depends on cell fault modes.
	"Lock" of BMS which requires intervention and correction to override	Depends on cell fault modes.

Design criteria	Considerations
Off-gas Monitoring integration into BMS	See Nexceris control logic (discussed in Section 1.4).
Shutdown criteria from OGM to BMS	See Nexceris control logic (discussed in Section 1.4).
Multi-functional intumescent material specifications	Depends on cell form factor, system weight requirements, system voltage, system dimensions, series-parallel cell configurations.
Intumescent material weight and dimensional constraints	Same as above
Venting/gassing channels based on cell form factor	Venting channels will be necessary to redirect gases away from neighboring cells. Containment of gases will lead to trapped explosive gases. They should be vented and directed away from neighboring batteries.
Thickness of walls	The exterior dimensions will determine how much intumescent materials can be fit into the module and system, and may also impact the selection of the cell form factor. The intumescent solution has been demonstrated with cylindrical cells, and will require special considerations for pouch or prismatic cells.

In addition, DNV GL has provided a common alarm, error, and fault response function list that is typical of most basic BMS. Table 10 shows the parameters, code descriptions, fail criteria, and corrective actions associated with each fault.

Table 10. Typical BMS fault response function list

Fault Code	Monitored Parameter	Code Description or Fault	Fail Criteria	Action
1	Cell Voltage	Battery Cell V Critical Low	V < Min V	Disconnect string and set current limits to 0
2	Voltage	Battery Cell V Low	V < Min V warning threshold	Disconnect string and set current limits to 0
3	Voltage	Battery Cell V Critical High	V > Max V	Disconnect string and set current limits to 0
4	Voltage	Battery Cell V High	V > Max V warning threshold	Disconnect string and set current limits to 0
5	Temperature	Battery Cell T Critical High	T > Max T	Disconnect string and set current limits to 0
6	Temperature	Battery Cell T High	T > Max T warning threshold	Disconnect string and set current limits to 0
7	Temperature	Battery Cell T Low	T < T_Min	Disconnect string and set current limits to 0

Fault Code	Monitored Parameter	Code Description or Fault	Fail Criteria	Action
8	Communication	Lost CAN Communication to Module	Delay > 3 sec	Disconnect string and set current limits to 0
9	Current	Battery String Over Current	Current > Current Max	Disconnect string and set current limits to 0
10	Communication	Lost CAN Communication to Cabinet Control Module	Delay > 3 sec	System Shutdown
11	Binary	Battery string Fuse Blowout	Fuse blow signal set to High	Disconnect string
12	Voltage difference between bus and string	Cabinet main negative relay weld	|Vbus - Vstr| < Low String V	Disable cabinet
13	Voltage difference between bus and string	Cabinet main negative relay failed OPEN	|Vbus - Vstr| > High String V	Disable cabinet
14	Voltage difference between bus and string	String Relay Weld (failed Short)	|Vbus - Vstr| < low string V	Disable cabinet
15	Voltage difference between bus and string	String Relay Failed OPEN	|Vbus - Vstr| > high string V	Disable string
16	Voltage difference between bus and Inverter input voltage	DC Breaker Weld (failed short)	|Vbus - Vinv| < low string V	System in IDLE mode
17	Voltage difference between bus and Inverter input voltage	DC Breaker Failed OPEN	|Vbus - Vinv| > high string V	System in IDLE mode
18	Binary	Smoke Alarm	Input high	System Shutdown + Remote Alarm
19	Binary	HVAC Alarm	input high	Remote Alarm
20	Temperature	Cabinet Control Box T High	T > Max T	System shutdown
21	Voltage difference between string and charger voltage	Charger Relay Failed OPEN	|Vstr - Vchg| > high V	N System shutdown

Fault Code	Monitored Parameter	Code Description or Fault	Fail Criteria	Action
22	Communication	Lost Communication to Inverter		Open DC Breaker
23	Voltage difference between string and charger voltage	Charger Relay Weld (failed CLOSED)	|Vstr - Vchg| < low V	Disable Charger

All of the following are determined by the cell chemistry:

V Max Warning – Determined by safety threshold lower than the max voltage of the cell. For example, if the cell maximum voltage is 4.2 V, the warning should be 4.1 V.

V Min Warning – Prior warning that the minimum voltage is being encroached; if V Min is 2.0 V, then warning at 2.05 or 2.1 V may occur.

V Max – The maximum voltage of the cell considered to be a critical fault. For example, if the maximum recommended electrochemical voltage of the cell is 4.2 V, this should be the critical voltage and V_{max}.

V Min – The minimum voltage of the cell considered to be a critical fault. For example, if the cell minimum is 2.0 V, then this should be the critical voltage.

T Max – The maximum tolerable temperature for the battery cells. If the battery cell becomes unstable at 60ºC, then this should be $T_{max,}$ with a safety buffer.

T Max Warning – A substantial buffer before T_{max} is reached, typically 5-10 ºC depending on the temperature fault tolerance of the battery chemistry.

T Min – Minimum tolerable temperature threshold that represents a shutdown to avoid critical failure.

T Min Warning – Prior warning that temperature is encroaching on critical temperature, typically 5-10º C of prior warning.

High String V – Dependent on series architecture of the string and the sum of min and max cell voltages. The max voltage will be proportional to the V Max Warning.

Low String V - Dependent on series architecture of the string and the sum of min and max cell voltages. The low voltage will be proportional to the V Min Warning.

TASK 4.4 – CAB ACCEPTANCE CHECKLIST

In all test cases, the cells should be properly conditioned (several charge/discharge cycles) to ensure there are no defects. Prior to all tests, it is anticipated that all cells should be brought to 100% state of charge (SOC). This is based on prior research relating to batteries commercially available today, wherein higher SOCs are associated with more complete failures. For yet not contemplated cell technologies, it may be valuable to characterize SOC influence on failure, with the most impactful scenario used throughout all future tests. Unless otherwise noted, all tests should occur in a reasonably standardized environment at approximately 1 atm, and recommended within 25% of 25 °C and 50% relative humidity. Consistency between tests should be prioritized over precision for a selected environmental condition. Cell characteristics should be known prior to any testing, including mass and voltage. In all cases, time series data should be collected, to allow comparison of critical parameters.

An example test procedure template for Thermal runaway/failure is provided below.

Test procedure template:

Purpose:

Demonstrate that the battery cannot go into thermal runaway regardless of external stimuli or, if it does, that it does not create a hazardous condition.

Required Materials:

1. Battery cells
2. Testing chamber, free of flammable or hazardous materials
3. External stimuli: Flexible film heater, mechanical stressor (e.g., nail gun), electrical connections, convective heat source, and/or controllable flame source (e.g. gas torch)
4. Detection technology, appropriate to the battery, at least: gas (flammability and toxicity), heat

Test Procedure:

1. Allow cell to rest for 1 hour, after bringing to 100% SOC (or selected SOC)
2. Apply external stimuli, one at a time, beginning with heat-sources. If an external stimulus does not have a measurable impact, perform a charge/discharge cycle to ensure fully operational prior to the successive test.
3. Repeat the test on two successive cells, for a total of three cells, to ensure repeatability of results.

Acceptance Criteria:

1. Battery does not reach go into thermal runaway, or
2. Battery does not release any flammable or toxic gases; does not release excessive heat (>65° C per RTCA standards); does not create any projectiles

Results template:

Product tested:		
Conducted By:		**Test Date:**
Test Notes:		
Step	**Units**	**Results**
Lab ambient	°C / RH % / atm	
Test 1		
Start time:	hh:mm	
SOC at test initiation	%	
Voltage at test initiation	V	

External stimuli used	Indicate all, with successful initiator specified by (*)	
Max external cell temp	°C	
Gases released	Name and ppm	
Observed flaming or projectiles?	y/n, description	
End time:	hh:mm	
Mass after test	g	
Voltage after test	V	
Test 2		
Start time:	hh:mm	
SOC at test initiation	%	
Voltage at test initiation	V	
External stimuli used	Only successful Test 1 stimulus	

Max external cell temp	°C	
Gases released	Name and ppm	
Observed flaming or projectiles?	y/n, description	
End time:	hh:mm	
Mass after test	g	
Voltage after test	V	
Test 3		
Start time:	hh:mm	
SOC at test initiation	%	
Voltage at test initiation	V	
External stimuli used	Only successful Test 1 stimulus	
Max external cell temp	°C	
Gases released	Name and ppm	

Observed flaming or projectiles?	y/n, description		
End time:	hh:mm		
Mass after test	g		
Voltage after test	V		
Pass / Fail:	Thermal runaway does not occur		□ Pass □ Fail
	No flammable or toxic gas release		□ Pass □ Fail
	No external temperatures exceeding 65°C		□ Pass □ Fail
	No projectiles		□ Pass □ Fail

TASK 4.5 – DELIVERY OF DESIGN PACKAGE TO CAB

Design Overview

The prototype system includes both active and passive systems to meet each design objective. The core system design centers on an intumescent block, with holes in which cylindrical Li-ion battery cells can be slotted, and lid to cover the tops of the cells. Inside this block are pathways for connecting wires and an attachment to an exhaust system, where off-gas monitor equipment is installed. Figure 23 shows a rendering of one version of this block.

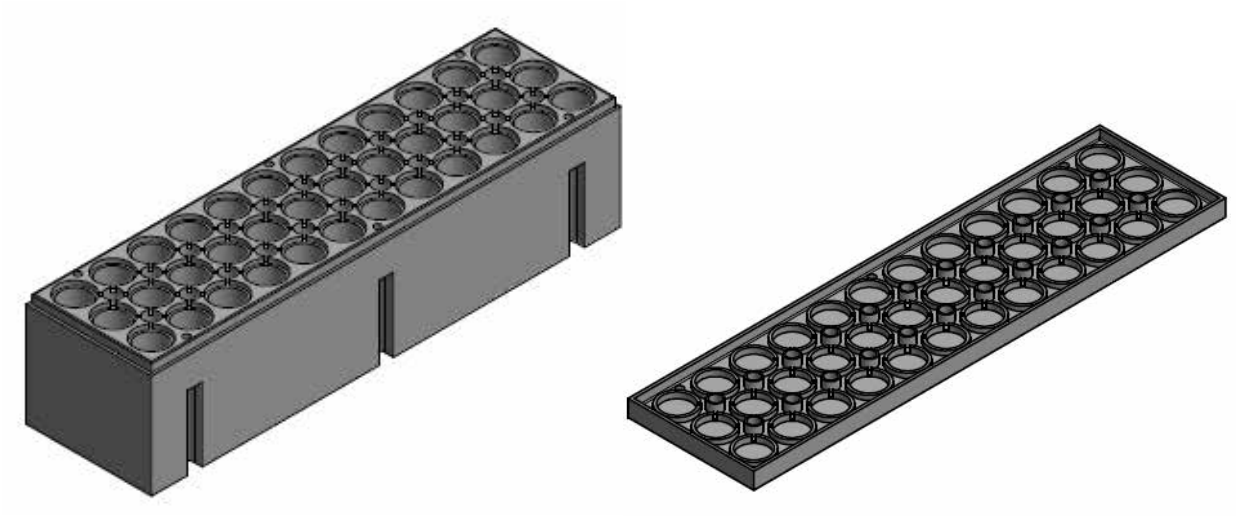

Figure 23. Intumescent cell block (left image, base; right image, lid)

The intumescent cell block was produced in two different designs, to determine which would more successfully reduce impact to cells adjacent to a cell under thermal runaway. In the Type 2 design (see Figure 24), the cells are lined up in three parallel rows of twelve cells each. As such, each cell has eight direct neighboring cells. In addition, the Type 2 block included small holes in the intumescent materials surrounding the center row, intended to facilitate movement of air in the block. In the Type 1 design (see Figure 25), the cells are arranged in three slightly offset rows of twelve cells each, allowing for a higher packing density while reducing the number of cells directly neighboring from eight to six.

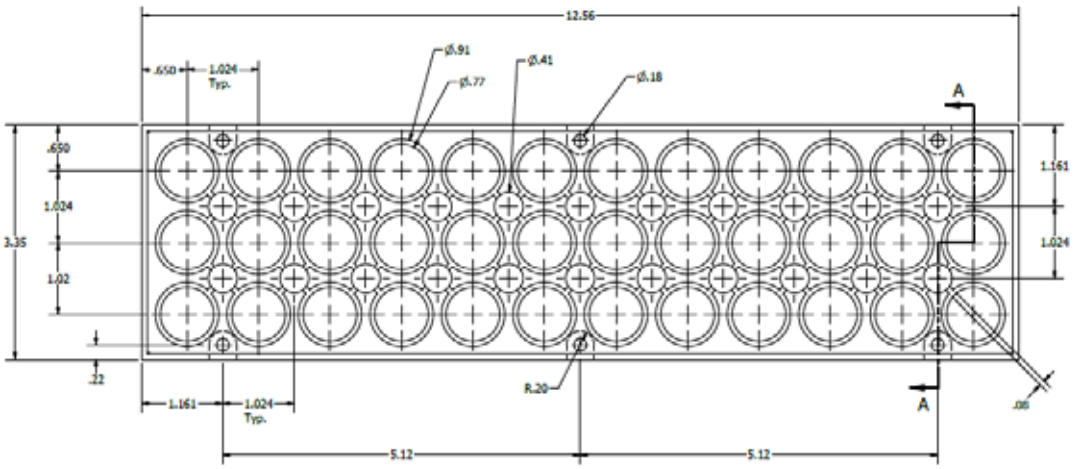

Figure 24. Type 2 configuration

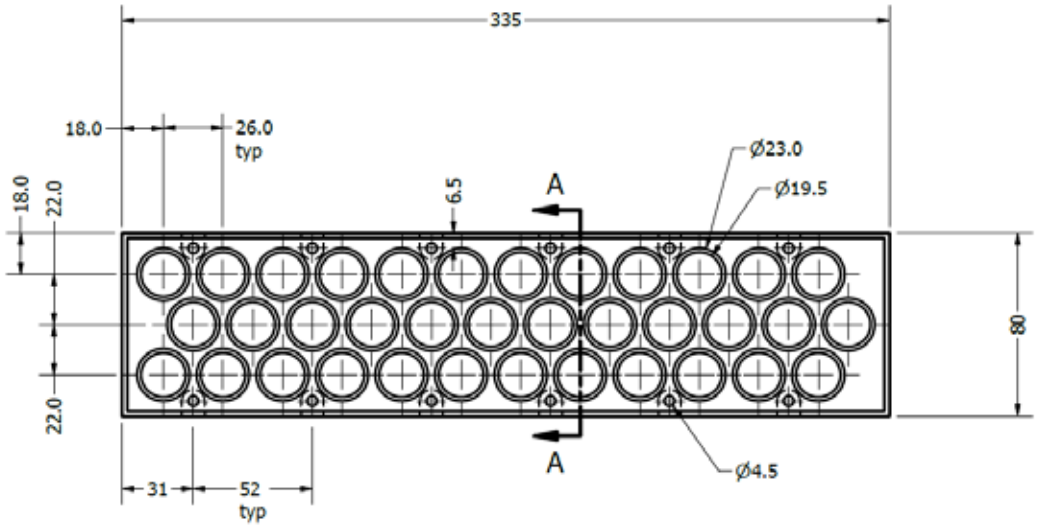

Figure 25. Type 1 configuration

This block is then placed inside of a metal casing, to fully enclose all the materials and serve as an exhaust manifold, with outlets for wires and airflow remaining. A rendering of the metal casing/exhaust manifold is provided in Figure 26, showing the top and bottom of the casing, inlet/outlets, gaskets, and screws/nuts.

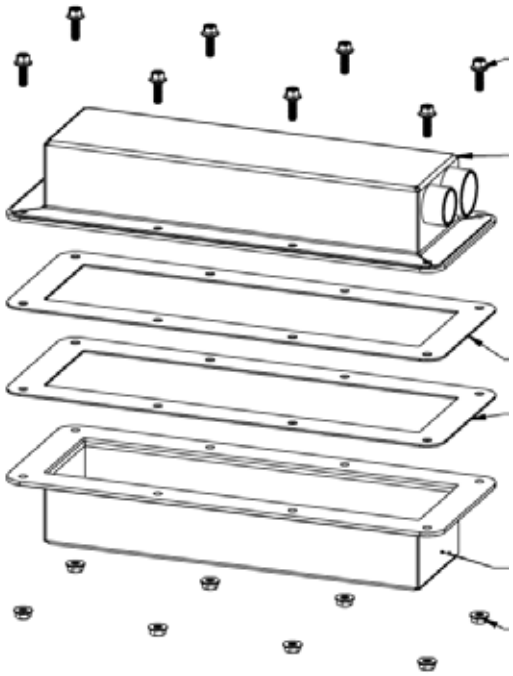

Figure 26. Metal casing/manifold

Cylindrical cells, as previously noted, are slotted into the block, and can be connected together in the desired parallel/series configuration appropriate to the application, with the DC output emerging from the casing. In addition, the exhaust manifold allows for the movement of air through the case, with an off-gas monitor included within the exhaust pathway. In the prototype, two different exhaust output piping was considered: one with a diameter of 1 inch, and the second with a diameter of ¾ inch. A single off-gas monitor was included for each test; however, in a real-world installation, fewer than one detection device per block may be acceptable in an interconnected, multi-block system. Additionally, in the prototype, no active exhaust was employed during testing, but, when scaled as part of a larger system, exhaust is anticipated to leverage the manifold design.

Finally, in the prototype, a battery management system was not directly included; rather, the off-gas monitor served to provide signals that would typically pass through the BMS to trigger a mitigative action. Inclusion of a BMS is required in the case of a full-scale demonstration.

System Subcomponents

Critical system subcomponents are noted in Table 11 below. This design list is intended to both provide a list of components to directly duplicate the design into production, and to provide

considerations for why the particular component was used, in order to guide decision making for the selection of alternative providers or technologies, as the design evolves.

Table 11. System subcomponents and support of design objectives

System component	Prototype supplier / model	Design objective	Considerations
Battery cell	26J cylindrical cells (18650) by Samsung	Resistance to thermal runaway; Prevention of cascading; Limitation/containment of external impact	Cylindrical cells include a passive failure system, where a cell under failure conditions will automatically disconnect from electrical connection, potentially preventing continued abuse conditions. Cylindrical cells allow, in the given packing format, a limited surface area for heat emanation to neighboring cells. Cylindrical cells limit energy density in comparison to prismatic or pouch cells, thus limiting impact of a cell runaway event. Differentiation between 18650 cells and 2170 cells was not considered. Other cell form factors may be considered, given these considerations are addressed in the design, either inherent to the cell or with additional or alternative protections. Cell chemistry/supplier was based on availability; differentiation of failures between cell chemistries/suppliers was not considered.
Battery block	IntuPlas by Pyrophobic Systems Ltd.	Prevention of cascading; Limitation/containment of external impact	The patented intumescent thermoplastic can be injection molded into a multitude of shapes and sizes, appropriate for the wide variety of forms that cells may take. The Type 1 block demonstrated a higher resistance to cascading failures, by reducing the number of exposed cells and eliminating the “tortured path” of the additional air holes in Type 2 design.

System component	Prototype supplier / model	Design objective	Considerations
Enclosure / Exhaust manifold	Custom enclosure by Endurance Engineering, Inc.	Resistance to thermal runaway; Prevention of cascading; Limitation/containment of external impact	The enclosure is intended to contain any failures internal to the block. The exhaust manifold supports rapid detection of failures in concert with the off-gas monitor equipment. The exhaust manifold can support removal of hazardous gases from the container, to limit impact within safe ranges. The 1-inch diameter exhaust outlet piping was found to provide improved temperature management. The custom-made enclosure was selected based on locally available resources.
Off-gas monitor	Li-ion Tamer by Nexceris	Resistance to thermal runaway; Prevention of cascading; Continuous monitoring	Incipient gas detection can support the prevention of thermal runaway, by detecting failures during the preventative region of cell abuse, and sending a signal to electrically disconnect the impacted cell or battery string. Off-gas monitoring, even if it cannot react rapidly enough to prevent thermal runaway in the initial cell, can serve to provide ‘early warning’ and limit cascading failures through the activation of selected mitigation system(s). Off-gas monitoring, paired with other BMS monitoring, should communicate status of the system to allow for safe operation or graceful shutdown.